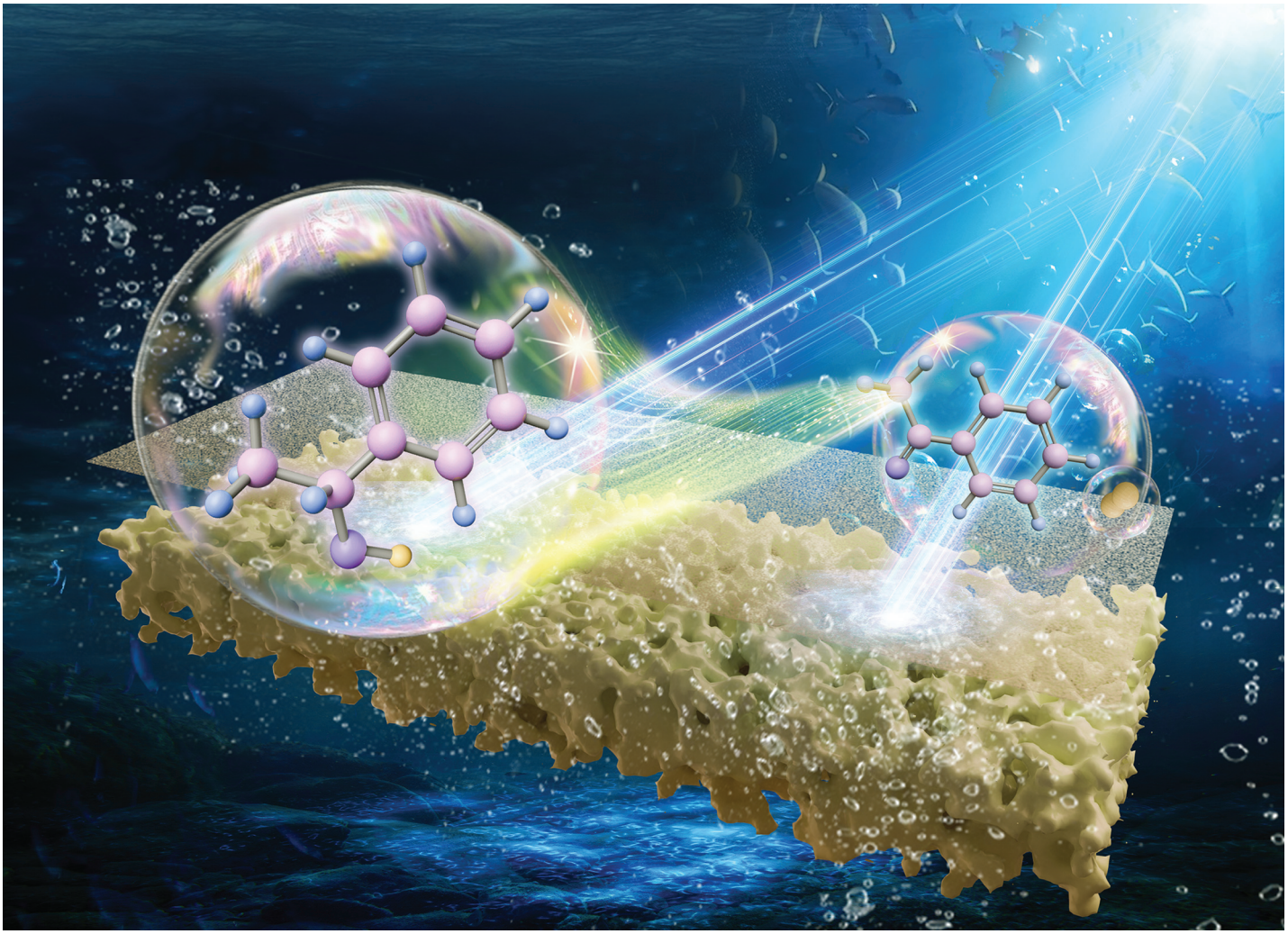

Showcasing research from Professor Abdi's laboratory, School of Energy and Environment, City University of Hong Kong, Hong Kong SAR, China.

Life cycle analysis of sustainable H_2 production and hydrogenation of chemicals in a large-scale coupled photoelectrochemical system

Pairing solar hydrogen production with the right chemical reactions is key to a negative carbon footprint. This integrated approach transforms the economics and sustainability of green hydrogen, paving the way for a solar-powered chemical industry. Careful pathway selection is essential for unlocking this potential.

Image reproduced by permission of Fatwa F. Abdi from *Green Chem.*, 2025, **27**, 12967.

As featured in:

See Fatwa F. Abdi *et al.*, *Green Chem.*, 2025, **27**, 12967.

ROYAL SOCIETY OF CHEMISTRY

rsc.li/greenchem

Registered charity number: 207890

Green Chemistry

PAPER

View Article Online
View Journal | View Issue

Cite this: *Green Chem.*, 2025, **27**, 12967

Life cycle analysis of sustainable H_2 production and hydrogenation of chemicals in a large-scale coupled photoelectrochemical system

Xinyi Zhang, [a,b] Michael Schwarze,[c] Ferry Anggoro Ardy Nugroho, [d,e] Muhammad Roil Bilad, [f] Carol Sze Ki Lin, [a] Reinhard Schomäcker, [c] Roel van de Krol [b,c] and Fatwa F. Abdi *[a]

Photoelectrochemical (PEC) water splitting is a potentially promising technology for renewable hydrogen production, addressing the growing demand for clean and sustainable energy sources. However, current PEC production of hydrogen is still not cost-competitive. A strategic approach to enhance the economic competitiveness of PEC-generated hydrogen is to couple it to selected homogeneous catalytic hydrogenation reactions to synthesize higher-value chemicals. Our previous studies have shown that combining PEC with these hydrogenation reactions effectively reduces the cost of hydrogen, but the lifecycle environmental impact of such a system is still unclear. In this study, we perform a life cycle analysis of a prospective large-scale coupled PEC hydrogenation system to evaluate its overall environmental impacts and compare them with the benchmark hydrogen production methods. Three coupled hydrogenation pathways were examined based on their previously demonstrated economic viability. Our results indicate that coupling hydrogenation reactions significantly mitigate the system's negative environmental impacts across its lifecycle, with the hydrogenation of itaconic acid to methyl succinic acid offering the highest reduction in cumulative energy demand (CED) and the addition of acetophenone to 1-phenylethanol hydrogenation demonstrating the most significant reduction of global warming potential (GWP). Notably, adding phenol-to-cyclohexanol hydrogenation, despite being economically attractive, produces higher environmental burdens, making it less favorable. Sensitivity analysis highlights the pivotal roles of solar-to-H_2 efficiency, H_2-to-chemicals conversion, and system longevity in reducing the system's environmental impact. Overall, our study emphasizes that careful selection of the coupled hydrogenation pathways can substantially enhance the sustainability of the PEC system and underscores the potential of integrated solar-driven hydrogenation processes.

Received 28th April 2025,
Accepted 27th August 2025

DOI: 10.1039/d5gc02117k

rsc.li/greenchem

Green foundation

1. This study employs thorough life-cycle analysis (LCA) to evaluate the environmental benefits of *in situ* coupling of photoelectrochemical (PEC) hydrogen production with selective hydrogenation reactions as a pathway to decarbonize chemical manufacturing.
2. Coupling hydrogenation reactions significantly reduces lifecycle environmental impacts compared to standalone PEC hydrogen production, with acetophenone hydrogenation showing the most substantial improvements. This LCA clearly advances over previous technoeconomic analysis work by quantifying for the first time the environmental trade-offs and identifying pathways that enhance both economic and ecological sustainability.
3. In future work, this LCA framework can guide the design of integrated PEC systems and inform research efforts toward more sustainable solar-driven hydrogenation processes.

[a]*School of Energy and Environment, City University of Hong Kong, 83 Tat Chee Avenue, Kowloon, Hong Kong S.A.R., China. E-mail: ffabdi@cityu.edu.hk*
[b]*Institute for Solar Fuels, Helmholtz-Zentrum Berlin für Materialien und Energie GmbH, Hahn-Meitner-Platz 1, 14109 Berlin, Germany*
[c]*Technische Universität Berlin, Department of Chemistry, Straße des 17. Juni 124, 10623 Berlin, Germany*
[d]*Department of Physics, Faculty of Mathematics and Natural Sciences, Universitas Indonesia, Depok 16424, Indonesia*
[e]*Institute for Advanced Sustainable Materials Research and Technologies (INA-SMART), Faculty of Mathematics and Natural Sciences, Universitas Indonesia, Depok 16424, Indonesia*
[f]*Faculty of Integrated Technologies, Universiti Brunei Darussalam, Gadong BE1410, Brunei*

Introduction

The rising anthropogenic carbon dioxide (CO_2) concentrations in the atmosphere due to the use of fossil-based resources have resulted in global warming and associated environmental issues. One of the most important strategies to tackle this enormous challenge is transitioning our energy use from fossil fuels to sustainable and renewable sources.[1] However, most renewable sources (*e.g.*, solar, wind) are inherently intermittent. Therefore, storage options are required to ensure a continuous supply of energy. Hydrogen has been considered a clean energy carrier due to its environmentally benign reaction with oxygen to release the stored energy, producing no downstream CO_2 emissions. In this context, storing renewable energy in the form of compressed hydrogen supports the integration of intermittent sources into the energy system. Depending on the availability, energy can be used immediately or delayed after its generation, providing flexibility to manage supply and demand. This flexibility offers additional degrees of freedom to use energy more efficiently, minimizing waste and maximizing the environmental benefits of renewables.

Unfortunately, hydrogen is currently produced almost exclusively from fossil fuels, primarily through steam methane reforming (SMR), which annually consumes 205 billion m^3 of natural gas and emits 820 Mt of CO_2.[2] To avoid these emission, renewable approaches to generate hydrogen have been considered. Table S1 in the Supplementary Information (SI) summarizes the global warming potential (GWP) of current hydrogen production methods, encompassing both renewable and non-renewable pathways. Among these, wind-powered electrolysis currently exhibits the lowest GWP (0.6 kg CO_2-eq per kg H_2).[3] Although the approach is at its nascent technological development phase, photoelectrolysis also promises low GWP and has been considered as a green and sustainable alternative to produce hydrogen from sunlight. In general, two approaches can be used: (i) indirectly by combining photovoltaic cells and electrolyzers (PV–EC) and (ii) directly in photoelectrochemical (PEC) cells. To this end, PV–EC systems are technologically mature, and up to 30% solar-to-hydrogen (STH) efficiencies have been demonstrated.[4] Meanwhile, the technological readiness level (TRL) of PEC systems is lower (TRL 3–5),[5] but laboratory-scale demonstrations have reported STH efficiencies up to ~20%.[6,7] Despite these encouraging achievements, implementing green hydrogen production from sunlight is still challenging due to its high cost. Several technoeconomic assessment (TEA) studies reported that the levelized cost of hydrogen (LCOH) from photoelectrolysis (either PV–EC or PEC) is expected to be ~6–10 USD per kg,[8–13] which is much higher than that produced from SMR (~1.4 USD per kg).

One approach that has been proposed to improve the overall competitiveness of solar-driven hydrogen is to integrate chemical synthesis within the same device. For example, researchers have considered replacing oxygen evolution with reactions that generate valuable chemicals from biomass-based or waste feedstocks (*e.g.*, glycerol oxidation, 5-hydroxymethylfurfural oxidation, lignin oxidation).[14–16] Alternatively, hydrogen generation can be coupled with its direct use or application in the same device. Such an integration potentially reduces the balance-of-system costs, and if the direct use of the generated hydrogen yields valuable products, the overall system competitiveness can be improved.[17] We have recently introduced and demonstrated the concept of coupling PEC hydrogen production and hydrogenation in a single device,[18] based on the Type 3 PEC configuration described by James *et al.*[19] In that system, PEC-generated hydrogen was used *in situ* for the coupled homogeneous hydrogenation reaction of itaconic acid (IA) to methyl succinic acid (MSA). A coupling efficiency (H_2-to-MSA conversion) of ~50% was demonstrated, *i.e.*, ~50% of the generated hydrogen molecules was directly used to hydrogenate IA to MSA, while the remaining ~50% was collected as gaseous hydrogen. A net energy balance assessment revealed that integration of the hydrogenation of IA to MSA within the PEC system improves the net energy balance and decreases the energy payback period.[20] In addition, TEA showed that the LCOH could be dramatically reduced by coupling PEC hydrogen production and hydrogenation, to a point that it becomes cost-competitive with hydrogen production from SMR.[18] The TEA study has been expanded recently to include other hydrogenation reactions. In addition to IA to MSA, coupling the hydrogenation of phenol to cyclohexanol and acetophenone (ACP) to 1-phenylethanol was found to impact the economic competitiveness positively by decreasing the LCOH.[17]

With the coupled PEC hydrogenation concept shown to be attractive from the net energy and economic perspective, its overall impact on the environment and resource utilization remains unknown. Therefore, in this study, we investigate how coupling the hydrogenation reaction inside a PEC hydrogen production system would affect its life cycle environmental impact. We consider three hydrogenation reactions that are potentially profitable: IA to MSA, phenol to cyclohexanol, and acetophenone to 1-phenylethanol (see Tables S2 and S3). Note that all the corresponding products find their use in various industrial-scale chemical processes and applications. A comparison between scaled-up systems (equivalent production of 1000 kg H_2 per day) that generate these different co-products is conducted to identify the most environmentally friendly option. Comparative analysis at much larger scale (equivalent to 50 000 kg H_2 per day) is also performed to investigate the impact of economies of scale; a recent study—albeit focusing on the Type 2 'Z-scheme' photocatalytic system instead of PEC—demonstrated that such a large-scale implementation could reduce the GWP per kg hydrogen by 18%.[21] Several assessment methods are utilized to calculate a total of 18 indicators, covering a diverse set of environmental impacts, ranging from climate change, ozone depletion, human health effects, and resource depletion. Finally, the environmental performance of the coupled processes is compared with benchmark figures of other competing hydrogen production methods, such as conventional SMR and PV–EC, to assess the implementation potential of the coupled reactions.

Methodology

LCA methodology

We followed LCA standards specified by the International Organization for Standardization (ISO),[22] ISO14040 and ISO14044, together with the principles and framework established by the Techno-Economic Assessment (TEA) & Life Cycle Assessment (LCA) Guidelines for CO_2 Utilization (version 1.1).[23] The guidelines provide a specific protocol for multi-functional carbon capture and utilization (CCU) plants, which was subsequently adapted for the PEC system in this study. A "cradle-to-gate" system boundary was adopted, in which the PEC-produced hydrogen and hydrogenated chemicals were assumed to be free of downstream emission after leaving the plant gate. All impacts related to raw materials, product manufacturing, and decommissioning were considered. This LCA is divided into four principal stages: (i) goal and scope definition, (ii) life cycle inventory (LCI), (iii) life cycle impact assessment (LCIA), and (iv) interpretation of results, as described in the following.

Goal and scope definition. The goal of this LCA is to assess the lifecycle environmental impacts associated with a prospective large-scale coupled PEC hydrogenation system that co-produces value-added chemical products, including MSA,[24–26] cyclohexanol,[27] and 1-phenylethanol.[28] The technical feasibility of performing hydrogenation reactions that generate these target chemicals at conditions relevant to PEC hydrogen production has been demonstrated in these literature. Fig. 1 presents the cradle-to-gate system boundary that was used for this LCA, encompassing raw material acquisition, reactor assembly, system operation, and end-of-life disposal. Similar to previous studies by Shaner *et al.*[8] and James *et al.*,[19] the scrap value and the disposal of the system were not considered. Since the PEC reactor area is an important metric used to quantify the scale of such systems, the functional unit (FU) of this LCA is defined as 1 m^2 of photo absorber. The life cycle impacts of the generated hydrogen and the hydrogenation products are expressed in the units of MJ kg^{-1} H_2 and MJ kg^{-1} chemical products, respectively. All data regarding the manufacturing of raw materials, assembly of PEC devices, and installation were derived based on average values in Germany. The electric-to-primary energy conversion coefficient was determined based on the default value found in the Ecoinvent database (version 3).[29] System components with significant impacts were then identified through sensitivity analysis to provide insights for further optimization.

Life cycle inventory (LCI). Practical life cycle data were gathered from both Ecoinvent v3.5 databases and the literature, or were calculated if the data for specific processes or materials were not available. Then, the product system was modelled based on the LCA goal and scope. The material and energy flows throughout the life cycle of the coupled PEC hydrogenation system, accounting for both raw material synthesis and device fabrication, are listed in Table S4. All the data were converted to conform to their predefined functional units. Most LCI data was extracted from the literature[17,20] and the Ecoinvent database[29] to build the target scenarios in SimaPro (v9.3.0.3). New processes were created in SimaPro where the data was not present in the database or could not be extracted from existing literature. The LCI data for specific production

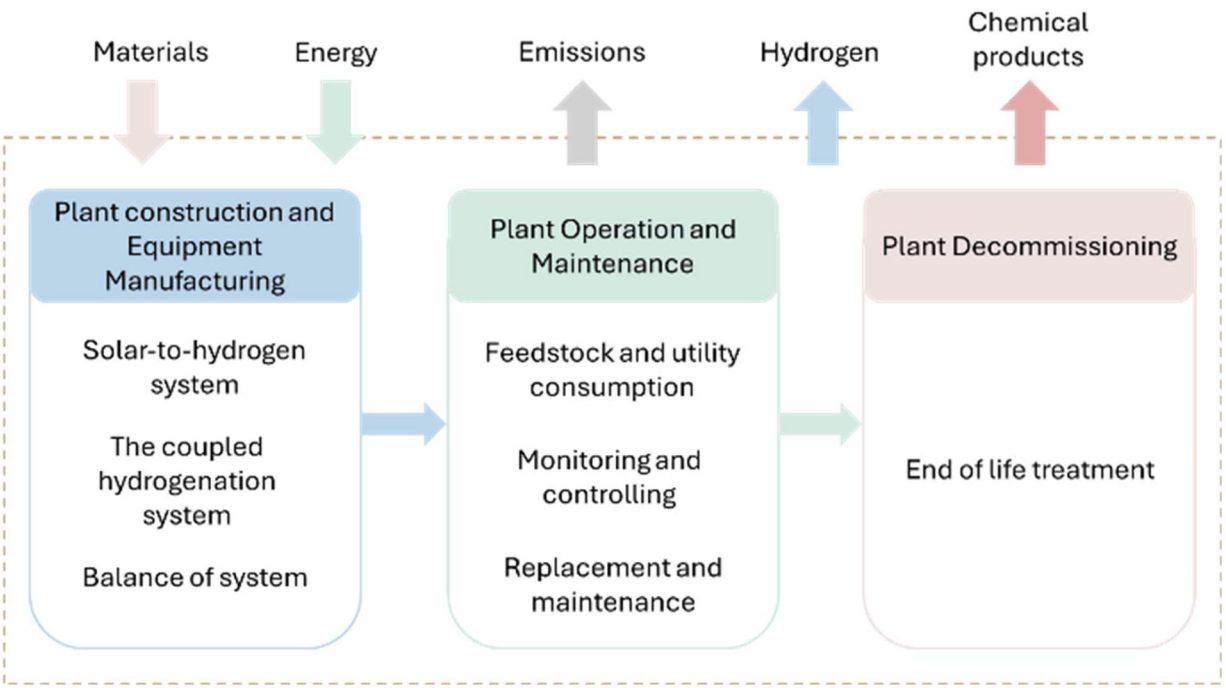

Fig. 1 Block diagram of the "cradle-to-gate" system boundary of the coupled hydrogenation PEC system considered in this study.

pathways were determined based on their respective synthesis mechanisms, the chemical and physical properties of the substances involved, and the associated energy consumption of the processing steps. For example, for the spray pyrolysis process of $BiVO_4$, thermodynamic modelling was performed using practical laboratory data and additional estimated parameters.[20]

Life cycle impact assessment (LCIA). The extensive input and output data from the LCI were systematically classified into relevant environmental impact categories. Emission flows identified during the inventory phase were assigned to one or more of these categories. For each category, the emissions were aggregated using characterization factors based on the chemical and physical properties of the respective substances. Several built-in LCA methods in SimaPro were applied, including cumulative energy demand (CED),[30] IPCC 2013 global warming potential (GWP) 100a,[31] and ReCiPe 2016 Midpoint (Hierarchist, H) impact assessment method,[32] to characterize the potential impact at the midpoint level. Each midpoint impact category comprises multiple indicators that quantify specific environmental mechanisms or processes within that category. To determine the ecological profile at the endpoint level, expressed as Eco-points, normalization and weighting were applied based on a hierarchist (H) perspective.

According to ISO 14044, three steps need to be considered for allocation. The first step (Step 1) suggests avoiding allocation by subdividing the system or expanding boundaries. This is not applicable in our case due to the inherent multi-product nature of our coupled hydrogen-hydrogenation system. Step 2 suggests physical allocation based on, *e.g.*, mass or energy content. As H_2 is not only a final product in our system but also an intermediate used for producing downstream chemicals, allocating impacts physically between H_2 and the hydrogenated product would be artificial and could misrepresent the process. Finally, Step 3 suggests the use of economic allocation based on the relative market value of each product. We also consider it less suitable as the prices of specialty chemicals can vary widely with time and region, introducing potential inconsistencies in the assessment. Given these considerations, our study applied a substitution method for product-specific impact assessments (as outlined in the Techno-Economic Assessment & Life Cycle Assessment Guidelines for CO_2 Utilization), considering the amount of environmental burden avoided by coupled hydrogenation (*versus* conventional hydrogenation) to offset the adverse impacts of the PEC system (Fig. S1a). Therefore, if the avoided burden from the hydrogenation products exceeds the overall impact of the system, the resulting impacts of hydrogen can even be negative. Eqn (1) and (2) were used to calculate the CED and the GWP per kg of H_2 produced from the PEC system once the substitution method was applied. The CED and GWP of the feedstocks and hydrogenation products were obtained from the literature or calculated using SimaPro based on their conventional manufacturing process. The specific process flow diagrams (PFD) outlining the major steps of device and system-level processing, which form the foundation for the SimaPro calculations, are depicted in Fig. S2.

$$\mathrm{CED}_{\mathrm{kg\_H_2}} = \frac{\mathrm{CED_{CAP}} + \mathrm{CED_{OP}} + \mathrm{CED_{DE}} - \mathrm{CED_{hydrogenation}}}{\Phi_{\mathrm{H_2\_collected}}} \quad (1)$$

$$\mathrm{GWP}_{\mathrm{kg\_H_2}} = \frac{\mathrm{GWP_{CAP}} + \mathrm{GWP_{OP}} + \mathrm{GWP_{DE}} - \mathrm{GWP_{hydrogenation}}}{\Phi_{\mathrm{H_2\_collected}}} \quad (2)$$

$\mathrm{CED_{CAP}}$ is the energy cost to construct the entire system, including all its components, $\mathrm{CED_{OP}}$ is the energy consumed during the system's operational lifetime, $\mathrm{CED_{DE}}$ is the energy cost for decommissioning, and $\mathrm{CED_{hydrogenation}}$ is the energy needed to produce hydrogenation products using their conventional manufacturing method (*i.e.*, the amount of energy that can be avoided if they were produced in a coupled PEC hydrogenation system). Similar definitions can be taken for the GWP parameters, except that they refer to the global warming potential instead of energy. $\Phi_{\mathrm{H_2\_collected}}$ is the amount of H_2 collected after the reaction.

Finally, while we do not consider the ISO 14044 Step 3 method (*i.e.*, economic allocation) preferable due to market volatility and uncertainty, we have also included it as a comparison in this study to provide a more comprehensive view of possible allocation outcomes. A schematic diagram of the method is shown in Fig. S1b.

Interpretation of results. The LCIA results of the coupled PEC hydrogenation system provide critical insights into the materials and process contribution to various environmental impact indicators in the interpretation stage. Prominent contributors to the overall impact were identified as environmental hotspots. Sensitivity analyses were then conducted to identify the most influential factors for further optimization. Based on this model, key parameters that can effectively reduce the overall emissions from PEC hydrogen production were identified. Various impact indicators (*e.g.*, global warming, particulate matter concentration, and acidification) were also included to ensure a holistic approach to the LCA and quantify the environmental impacts of renewable production of value-added chemicals.

Description and assumptions of the PEC facility

The engineering design of the employed plant-scale system was derived from the technoeconomic guidelines outlined in the US Department of Energy (DOE) Task 5.1 report on PEC hydrogen production systems.[19] Modifications (*i.e.*, additional separation facility, piping connections, *etc.*) were made to accommodate the coupling of our PEC process with a catalytic hydrogenation reaction, adjusting key design aspects to suit this integrated approach. Furthermore, several parameters were updated to reflect the specific geographic and temporal conditions considered in our study, including solar resource data from the European Commission's Photovoltaic Geographical Information System (PVGIS) in 2024.[33,34] Additional region-specific factors, such as European water[35] and electricity tariffs,[36] as well as market prices for precious

metals, were also incorporated into the model.[37] This study assumed that electricity for system operation would be supplied from the German electricity grid, which features a diverse energy mix of renewable and non-renewable sources. In 2024, approximately 60% of electricity generated in Germany was derived from renewable energy sources.[38]

The base case scenario of the coupled PEC hydrogenation system scale is described by the following main parameters: (i) an STH efficiency of 10%, (ii) a lifetime of 20 years, and (iii) a H_2-to-chemicals conversion coefficient of 10% (*i.e.*, when the system is co-producing hydrogenation chemicals). In this study, faradaic efficiency (FE) is considered when calculating the hydrogen production at the electrode, which should not be confused with H_2-to-chemicals conversion. The latter describes the fraction of hydrogen (generated at the electrode) that is directly utilized in the coupled hydrogenation process. Different values of FE are considered in the sensitivity analysis section for different hydrogenation reactions based on the reported literature. For example, Obata *et al.* have reported a FE close to 100% in their study on itaconic acid to methyl succinic acid conversion.[39] However, for the hydrogenation of phenol to cyclohexanol and acetophenone to 1-PE, the reported FE is only 70% and 76%, respectively.[40,41] Additional baseline production parameters are listed in Table S5. In particular, the assessed co-generation scenario is based on a hypothetical large-scale PEC facility with 1000 kg H_2 per day production capacity. The fixed flat panel array design was adapted from the Type 3 PEC configuration reported by James *et al.*[19] Ravilla *et al.* also reported the Type 3 configuration which facilitates comparative LCA between our coupled PEC hydrogenation system and prior research.[42] The construction of the PEC device is derived from our previously reported 50 cm^2 demonstration devices,[43] comprising a $BiVO_4$ top absorber, a silicon heterojunction (SHJ) bottom absorber, a deposited platinum catalyst, an ion exchange membrane, as well as separate inlets and outlets for unassisted solar water splitting.[20] Fig. 2a presents the simplified schematic configuration of the PEC device. The homogeneous catalyst and feedstock are dissolved in the catholyte (*i.e.*, an aqueous solution of potassium phosphate). Within the cell, the coupled hydrogenation reaction occurs in the catholyte compartment, where the generated H_2 hydrogenates substrates to valuable chemical products with the assistance of the homogenous catalyst. For all investigated coupled hydrogenation reactions, we assumed the use of the same homogeneous catalyst, *i.e.*, Rh-TPPTS, with the same concentration. Although each reaction would typically require different catalysts and concentrations, this assumption simplifies calculations, as the resulting impacts exhibit minimal sensitivity to catalyst variations. Finally, the device is assumed to degrade at a constant annual rate of 1% throughout its operational lifetime.

Fig. 2b shows the structure of a PEC panel, which is assumed to be fixed at an optimum tilt angle throughout the year, with each panel comprising multiple cells. The panel framework was adapted from the report of Sathre *et al.*[44] The PEC array including balance-of-system (BOS) is shown in Fig. 2c, and the baseline system layout (Fig. 2d) has a total 118 778 m^2 capture area

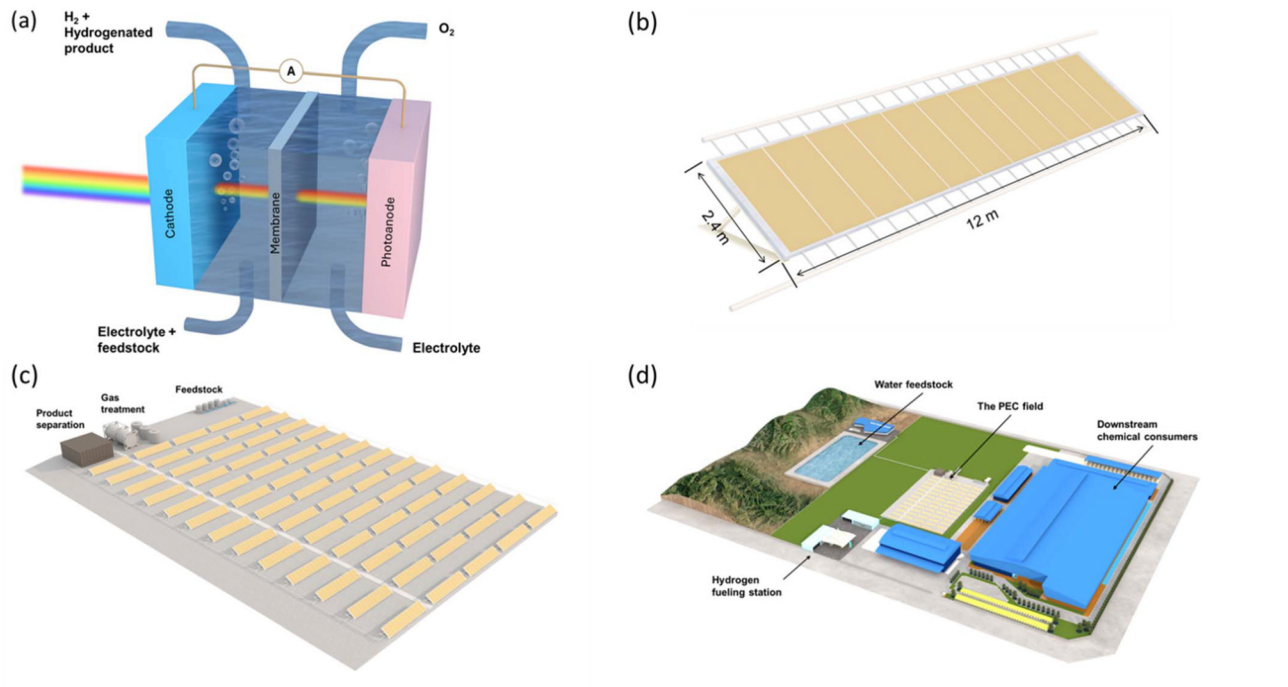

Fig. 2 Schematic illustration of the 1000 kg H_2 per day production PEC system at different levels: (a) photoelectrochemical cell with coupled hydrogenation. Here, H_2 generated at the cathode is utilized directly to hydrogenate feedstock to valuable product with the help of homogeneous catalyst dispersed in the catholyte. Illustrations of the corresponding (b) PEC panel, (c) PEC array layout and (d) facility layout are also shown. The facility is depicted to be located close to the applications (*i.e.*, H_2 fuelling station and downstream chemical consumers) for visualization purpose.

(corresponding to 59 389 panels of 1 × 2 m^2, and 60 arrays each containing approximately 1000 panels). The layout of the array and the entire facility followed a large-scale energy balance study[44] with additional facilities for feedstock and product separation. Each array was assumed to be equipped with gas compression and storage infrastructure for the daily production of H_2. Furthermore, adjacent panels are positioned with an end-to-end spacing of 0.5 meters and the spacing between rows of panels was set to be 6 meters based on a 10° tilt angle[45] to mitigate shading losses due to adjacent panels when the sun is low in the sky. Last, this study models a hierarchical network of conduits to transport gas and fluids.

For PEC systems with coupled hydrogenation reactions, additional pipe networks were included for the delivery of the products to the separation facility. The schematic diagram of the coupled PEC hydrogenation system in this study is shown in Fig. S3, which illustrates the connections between system components and flows. Within the system, it is assumed that 90% of the total surface area of the panel is the active solar collection area, and the remaining 10% is inactive due to structural or other requirements.[19,44,46] Since the size of individual cells does not significantly influence the overall impact of a panel, the panel was assumed to comprise multiple PEC cells ranging from 50–100 cm^2 which represents one of the largest cell sizes reported to date.[43] The device performance and operational parameters were used to determine the annual amount of hydrogen produced by the PEC system ($\Phi_{H_2\_produce,i}$ in kg) according to the following equation:

$$\Phi_{H_2\_produced,i} = \frac{I_{sunlight} \times \eta_{STH} \times 365 \times A_{active} \times \phi}{LHV_{H_2}} \quad (3)$$

where $I_{sunlight}$ is the solar intensity (3.43 kWh m^{-2} day^{-1}, the average value over the whole year for Germany), η_{STH} is the STH efficiency, A_{active} is the active area, ϕ is the system capacity factor (we assume 90% of the panels are working on average during the operation time) and LHV_{H_2} is the lower heating value of H_2 (33 kWh kg^{-1} or 120 MJ kg^{-1}). Note that the system capacity factor used in this study should not be misunderstood as the more common PV capacity factor.

The percentage of the *in situ* generated H_2 consumed to generate value-added products is defined by the H_2-to-chemicals conversion coefficient (μ). Our different assessment scenarios considered μ from 0% to 60%, but the base-case value was assumed to be 10%, which has been reported experimentally[18] and at which the system can also reach favourable economic conditions.[17] The amount of H_2 consumed ($\Phi_{H_2\_consumed}$) in the reaction is a product of μ and the amount of H_2 produced on the cathode ($\Phi_{H_2\_produced,i}$) (see eqn (4)).

$$\Phi_{H_2\_consumed,i} = \mu \times \Phi_{H_2\_produced,i} \quad (4)$$

The amount of H_2 collected after the reaction ($\Phi_{H_2\_collected}$) is calculated by eqn (5):

$$\Phi_{H_2\_collected,i} = (1 - \mu) \times \Phi_{H_2\_produced,i}. \quad (5)$$

And the annual amount of hydrogenation products generated ($\Phi_{hydrogenation,i}$) and feedstocks consumed ($\Phi_{feedstock,i}$) can be determined using eqn (6) and (7), respectively:

$$\Phi_{hydrogenation,i} = \frac{\Phi_{H_2\_consumed,i}}{M_{H_2}} \times M_{hydrogenation} \times \frac{\nu_{hydrogenation}}{\nu_{H_2}} \quad (6)$$

$$\Phi_{feedstock} = \frac{\Phi_{H_2\_consumed,i}}{M_{H_2}} \times M_{feedstock} \times \frac{\nu_{feedstock}}{\nu_{H_2}} \quad (7)$$

where M_{H_2}, $H_{hydrogenation}$ and $M_{feedstock}$ are the molecular masses of H_2, the hydrogenation product and the feedstock, respectively. ν_{H_2}, $\nu_{hydrogenation}$, and $\nu_{feedstock}$ are the stoichiometry coefficients for H_2, the hydrogenation product and the feedstock, respectively (see Table S2).

System energy and material flows

PEC reactor subassembly. The energy and materials consumed to manufacture the system components were calculated based on both experimental data and available literature. Energy requirements for producing the cells, including material sourcing and cell manufacturing, are based on our previous net energy balance analysis.[20] By dividing the total impact by the total product yields, the impact of subassembly was translated into the equivalent impact per unit product. $Impact_{cell}$, which is the primary impact of the PEC cell, was calculated based on a bottom-up approach from the impact of each part and subpart (see eqn (8)):

$$Impact_{cell} = \sum I_{material} \times W_{material} + \sum I_{utility} \times W_{utility} + I_{equipment} \quad (8)$$

where $I_{material}$ is the impact, *i.e.*, CED or GWP, of raw materials (kWh kg^{-1} H_2 or kg CO_2-eq per kg H_2), $W_{material}$ is the amount of material used (kg m^{-2}), $I_{utility}$ is the impact of the electricity (kWh kWh^{-1}, kg CO_2-eq per kWh) or water (kWh m^{-3}, kg CO_2-eq per m^3), $W_{utility}$ is the amount of electricity and water used (kWh m^{-2} and m^3 m^{-2}), $I_{equipment}$ is the equivalent CED or GWP of the equipment to produce a unit area of a cell over its entire lifetime (kWh m^{-2} or kg CO_2-eq per m^2).

The bottom absorber of the coupled PEC device examined in this study features a silicon heterojunction (SHJ) cell manufactured without front metal contacts. A study by Louwen *et al.* reported an emission of 20 g CO_2 eq. per kWh for the SHJ cell in their LCA.[47] Here, this number was re-evaluated for a single-sided metallized SHJ cell by excluding half of the materials and energy allocated to the metallization process.

The $BiVO_4$-based photoanode top absorber was taken to be directly deposited on the indium tin oxide (ITO) layer of the SHJ cell. The material consumption and fabrication steps were derived from our prior work on spray-pyrolyzed $BiVO_4$.[48] Currently, industrial-scale data is unavailable for fabrication of the $BiVO_4$ layer. Thus, the energy consumption and emission associated with this process were estimated based on the laboratory-scale fabrication conducted in our lab by applying an additional exponential scaling-up factor of 0.5.[19]

The oxygen and hydrogen evolution catalysts, namely, 30 nm cobalt phosphate (Co-P_i) and 20 nm Pt, were assumed to be electrodeposited onto $BiVO_4$ and solar-grade glass, respectively. The reported energy usage for the electrodeposition of thin film coatings is 1.54 kWh m^{-2},[49] which includes the energy used during the dipping (0.125 kWh m^{-2} min^{-1}), rinsing, drying, and calcination steps. In this study, a 15-minute dipping treatment was assumed. The estimated primary energy requirements for the electrodeposition of Co-P_i and Pt are 20.1 MJ m^{-2} and 13 MJ m^{-2}, respectively.[50]

Nafion (CF_2═CFO–C_3F_6–O–C_2F_4–SO_2F) was assumed to be the ion-conducting, gas-impermeable membrane in the PEC device. Due to the absence of this material in the Ecoinvent database, a new model was established in SimaPro to simulate the step-by-step synthesis process described by Duclos *et al.*:[51] (i) copolymerization of tetrafluoroethylene and a perfluoroalkyl sulfonyl fluoride,[52] (ii) an industrial scale extrusion process, and (iii) hydrolysis of the sulfonic groups with a hot solution of sodium hydroxide (NaOH) or potassium hydroxide (KOH) and conversion of the ionomer by a strong acid, such as nitric acid (HNO_3).

A transparent glass cover and a PVC chassis were considered for the device encapsulation. The energy consumption and emission associated with ancillary processes, including miscellaneous chemicals,[53] water pumping and cleaning,[54] and environmental control of the manufacturing facilities,[55] were disaggregated from existing PV-related LCA studies. The PEC reactor subassembly incorporates feedwater pumps and manifold pipes made from poly vinyl chloride (PVC), which transport electrolytes and liquid products in the system. The lengths of various pipes sizes were recalculated from the DOE report based on the facility parameters.[19] Detailed information regarding the energy and materials consumption for fabricating and installing the PEC reactor was adopted from our previous study.[20]

Balance of system (BOS). The PEC panels include a structural frame for mounting multiple PEC cells, onboard monitoring and diagnostics sensors, and pipe manifolds for delivering fluids to and from each cell. To anticipate the possibility of electrolyte leakage, low-density polyethylene (LDPE) tanks were assumed to be installed under each individual panel.[56] Considering all panel components, the total weight is estimated to be 720 and 1300 kg without and with electrolyte, respectively.[44] The transportation of panels from the factory to the facility is also included, assuming a 300 km truck transport.[44] Every ten years (replacement cycle), the panels will be dismantled from the array, and new components (PEC cells, manifolds, sensors) will be installed in the same steel framework.

We assumed deionized water as the electrolyte and the thickness of the two chambers containing electrolyte within the PEC cells is 1 cm.[57] Each panel contains approximately 540 liters of electrolyte, contributing to a total of 820 000 m^3 of electrolyte within the entire facility. A water treatment facility employing a reverse osmosis/electrodeionization (RO/EDI) method provides the daily water supply.[58,59] The facility capacity supports a peak water flow rate of 2 m^3 per hour for the entire system.[44] The water supplied for PEC production must meet high purity standards, with a resistivity >1 MΩ cm at 25 °C and minimum ion concentration to prevent contamination of the electrochemically active surfaces. The consumption of utilities, chemicals, and other consumables utilized throughout the RO/EDI process has been accounted for in the operations and maintenance (O&M) section.[58] Additionally, the waste management of the RO concentrate has been considered, resulting in an added energy consumption and emission for treated water.[60] This study focuses solely on the energy and material consumption associated with the water treatment process, assuming that the embodied energy of the RO hardware is negligible. Water usage during the hydrogen production process was calculated based on stoichiometric requirements, along with an additional 1% evaporation factor. Furthermore, it is estimated that 25 liters per year per m^2 of water will be consumed for the cleaning of the panel surface, this value is derived from a utility-scale photovoltaic systems.[61] Water pumps were assumed to operate only during the hydrogen production phase and for several hours thereafter. The water feed is managed using industrial electric water pumps,[62] with energy consumption estimated based on values reported by Plappally *et al.*[63]

The gas handling system consisting of PVC piping, blowers, a 2-stage gas compressor, and a condenser/cooler was assumed to be employed to collect, compress, separate and deliver the H_2 gas produced to the collection station/pipeline, operating at 1200 liters per min under peak H_2 production. The compressor's capacity is sized based on the maximum annual hydrogen production, coinciding with periods of maximum solar irradiance, and it operates at a reduced capacity on days with lower production. The condenser/cooler unit lowers the gas temperature and removes water vapor before the gas enters the compressor. Electricity consumption for gas handling is based on literature from industries and calculations.[64] Through the 300 km pipeline, a pressure drop of the gas is expected, and finally re-compression to 300 psi for delivery also requires additional energy input. The energy content (*i.e.*, the energy usage during the manufacturing process of the device) of the gas blower, dryer, and compressor hardware is based on Koornneef *et al.*,[65] assuming linear scaling with capacity.

In addition, on-site storage was implemented to buffer intermittent diurnal production and enable on-demand H_2 production similar to SMR. The maximum storage capacity for daily production was considered when calculating the storage capacity for H_2 and chemical products.[66] For H_2 storage, the calculation of the capacity using the ideal gas law leads to the storage volume needed for 1000 panels (one field) being about 300 m^3 at 300 psi at a temperature of 20 °C. Type I compressed hydrogen (CH_2) storage tanks were assumed to be utilized on site, made of carbon fibers and epoxy resin, and sized and designed according to Peters *et al.*[67,68] Sensitivity parameters include allowable metal stress, corrosion allowance, and valves and fittings allowance. For chemical storage, high-density poly-

ethylene (HDPE) and low-density polyethylene (LDPE) containers are used to store dry powder chemicals and the associated LCI data was derived from Treenate *et al.*[56]

The envisioned monitoring system consists of multiple sensors at the panel, array, and facility level, including temperature, pH, pressure, and flow sensors. These sensors transmit data to a central control center *via* a wireless network. Facility operations require mobile cranes and flatbed trucks operating 12 hours a day for maintenance, such as replacing cells or panels at the end of their service life. The LCI of the manufacturing process was recalculated in SimaPro based on an LCA study for automobile technologies.[69] In the sensitivity assessment, gasoline, hybrid, and electric vehicles were evaluated for different cases and energy consumption during the operational process is based on their specific machine ratings. Ancillary maintenance of equipment and infrastructure (*e.g.*, painting) was deemed negligible, therefore it was not included in the analysis.

Panel heating was also considered to avert device failure arising from the electrolyte freezing in cold weather. The freezing temperature of aqueous electrolytes is 0 °C and the lowest temperature in Berlin during winter was assumed to be about −10 °C.[70] To prevent electrolytes from freezing, each panel is equipped with an electrically powered strip heater. These heaters would operate based on feedback from embedded temperature sensors, activating when heating is needed. Detailed heating energy calculations are shown in Note S1.

At the end of the facility's lifetime, it would be decommissioned. This process includes systematic dismantling, remediation, and disposition of the facility's infrastructure and equipment through safe recycling or disposal methods. This study follows the method used in the series of energy system life cycle assessments summarized by the National Energy Technology Laboratory (NETL),[71] which assumes that decommissioning requires 10% of the energy expenditure consumed in the initial construction of the facility BOS.

Components for H_2-to-chemicals processes. Several types of feedstocks were utilized in this study, and the transportation distance from the source to the site was assumed to be 100 km for the base case. The energy consumption and emissions associated with feedstock delivery were calculated using built-in processes in SimaPro. Before feeding the catholyte into the PEC reactor, the feedstocks and homogeneous catalyst are dissolved in a continuous stirred tank reactor (CSTR).[72,73] The feedstock consumption in the coupled hydrogenation reaction was calculated according to the stoichiometric relationship between the feedstock and hydrogen, as listed in Table S2, and the H_2-to-chemicals conversion efficiency. The concentration of the homogeneous Rh-TPPTS catalyst is assumed to be 0.9 mM for all hydrogenation reactions. Theoretically, the Rh-TPPTS catalyst would not be consumed during operation. However, an annual loss rate of 1.2% was assumed in practical production, in line with the replacement rate of the PEC reactor.

The system was assumed to operate until the coupled hydrogenation reaction reaches the pre-set conversion efficiency, which is controlled by adjusting the flow rate.[18] Afterward, the resulting mixture—comprising catholyte, feedstocks, homogenous catalyst, H_2 gas, and hydrogenation products—is transferred to a separation facility. Compressed H_2 gas is collected and delivered to pipelines, while the remaining liquid mixture is processed in the separation unit to extract chemical products. Recent separation techniques, such as micellar-enhanced ultrafiltration and cloud point extraction, have been reported for separating IA, MSA, and the homogenous catalyst.[74,75] Conventionally, the catalyst is filtered off, and suitable acids (*e.g.*, hydrochloric acid, sulfuric acid) are added to extract MSA from its metal salt.[76] However, because these methods have not yet been commercialized, the separation process of succinic acid (SA) from conventional fermentation products was adopted as a proxy for base-case chemical separation.[77] It was reported that the downstream separation and purification account for approximately 16% of the total cost in the production of SA. This ratio is applied in our study to estimate the energy and material consumption associated with chemical separation. Moreover, since MSA exists primarily in the form of metal salts—specifically potassium methyl succinate due to the presence of potassium ions in our considered KPi electrolyte—further recovery of MSA necessitates acid treatment. This process typically involves the use of sulfuric acid or similar acids, resulting in additional chemical costs and increased post-treatment expenses. Therefore, the environmental and economic impacts associated with the separation process are expected to increase, and we further examine them through sensitivity analysis.

Results and discussion

Single-issue analysis

We begin our study by analysing three prevailing single-issue impact indicators in the LCA study of the projected coupled PEC hydrogenation system, *i.e.*, (i) the primary energy consumption (MJ m^{-2}), (ii) the global warming potential (GWP) per unit area of system (kg CO_2-eq per m^2) and per kg of hydrogen (kg CO_2-eq per kg H_2), and (iii) the cumulative energy demand (CED) per kg of hydrogen (MJ kg^{-1} H_2), according to the approach and boundary conditions described in the Methodology section. For the base-case scenario, the primary energy consumption of the coupled PEC hydrogenation system is 17 908 MJ m^{-2}. Fig. 3a shows the distribution of the contributing factors to the total primary energy consumption, with PEC reactors (including replacement of PEC cells) consuming approximately 40% of the total. This high percentage is mainly from substantial materials and energy inputs in the fabrication of the PEC cell, especially the energy-intensive process of purifying silicon to solar grade quality, which accounts for 90% of the total energy required for SHJ cell production.

The next largest energy consumers are panel heating and hydrogenation products separation, which account for 18.6% and 17.6% of the total energy consumption, respectively. This is not too surprising, as electric heaters consume a large

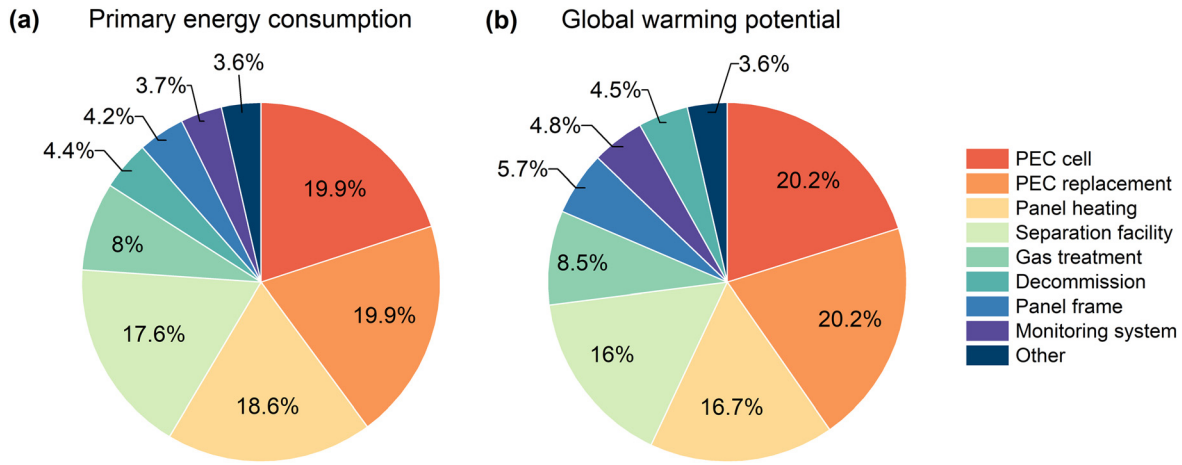

Fig. 3 Breakdown of the single-issue impacts of the system components within a base case coupled PEC hydrogenation system throughout its life-cycle: (a) primary energy consumption (MJ m^{-2}) and (b) global warming potential per unit area (kg CO_2-eq per m^2). For comparison, similar charts for a PEC system producing only H_2 are provided in Fig. S4.

amount of utility power from the electricity grid. Thus, for plant sites located in warmer regions where temperatures would not drop below the freezing point of electrolyte, it is expected that the elimination of energy consumed in the panel heating would effectively reduce the overall primary energy consumption. Chemical separation also requires a lot of absorbent material and chemicals during processing, contributing significantly to the primary energy consumption. Gas utilization and treatment constitute approximately 8% of the overall energy consumption. In contrast, processes such as decommissioning, the panel frame, the monitoring system, and the other BOS components (*i.e.*, the pumping and piping system, water supply, and facility operation) contribute in comparable proportions, each encompassing approximately 4% of the total.

The GWP of the coupled PEC hydrogenation system over its 20-year lifetime is calculated to be 1.2×10^8 kg CO_2-eq, which is equivalent to ~1011 kg CO_2-eq per m^2. Fig. 3b shows how much the individual components and processes contribute to the combined GWP of the entire system. Notably, PEC reactors (40.4%), panel heating (16.7%), the separation facility (16%), and gas treatment (8.5%) emerge as the top contributors, while the rest of system components collectively contribute to 18.5% of the total GWP. In contrast to the primary energy consumption (*cf.* Fig. 3a), the global warming impacts of the panel frame and the monitoring system surpass that of the decommissioning process due to the large percentage of metals and electronics usage. More detailed illustrations of the contributors to the primary energy demand and GWP of the coupled PEC – IA-to-MSA hydrogenation system are shown by the Sankey diagrams (see Fig. S5), built based on the hierarchy models in SimaPro.

For comparison, the primary energy consumption and the GWP of the PEC system that only generates H_2 were also calculated, which are 13 708 MJ m^{-2} and 770 kg CO_2-eq per m^2, respectively. These values are understandably lower than the coupled PEC hydrogenation system due to the absence of the homogeneous catalyst and the hydrogenation product separation components. Other than these exceptions, the overall distribution of the contributing factors is similar, as shown in Fig. S4.

To compare across different chemical products-generating PEC systems, the single-issue impact indicators per kg of hydrogen produced during the entire lifecycle were calculated. When the PEC system only generates hydrogen (*i.e.*, no coupled hydrogenation), the resulting cumulative energy demand (CED) is 223 MJ kg^{-1} H_2 (Fig. 4), comparable to a value previously reported for a large-scale hypothetical PEC water-splitting facility (*i.e.*, 214 MJ kg^{-1} H_2).[44] This energy demand is higher than the energy content of the hydrogen gas itself, as the lower heating value (LHV) is 120 MJ kg^{-1} H_2. In other words, the total energy harnessed from solar energy by the PEC system in this study is lower than the energy required for constructing and operating the system. Consequently, the system cannot repay its energy consumption if it produces only hydrogen. Moreover, our system requires more energy than current benchmark methods of hydrogen production, either fossil- (SMR) or renewable-based (*i.e.* wind and electrolysis). SMR has been reported to have an energy cost of 183.2 MJ kg^{-1} H_2,[78] while coupling wind turbines with electrolyzers to generate renewable hydrogen only requires 9.1 MJ kg^{-1} H_2.[79] Thus, H_2 derived from the PEC approach is not yet energetically on par with these alternatives.

Fig. 4 shows the CED of coupled PEC hydrogenation systems. Adding the coupled hydrogenation feature to the PEC system means more energy would be consumed during the entire lifecycle due to the inclusion of feedstock and separation facility. For the three studied hydrogenation reactions (*i.e.*, IA to MSA, phenol to cyclohexanol, and acetophenone to 1-phenylethanol), the CED values increased to 329, 270, and 1072 MJ kg^{-1} H_2, respectively. The coupled PEC hydrogenation system that produces 1-phenylethanol has a significantly

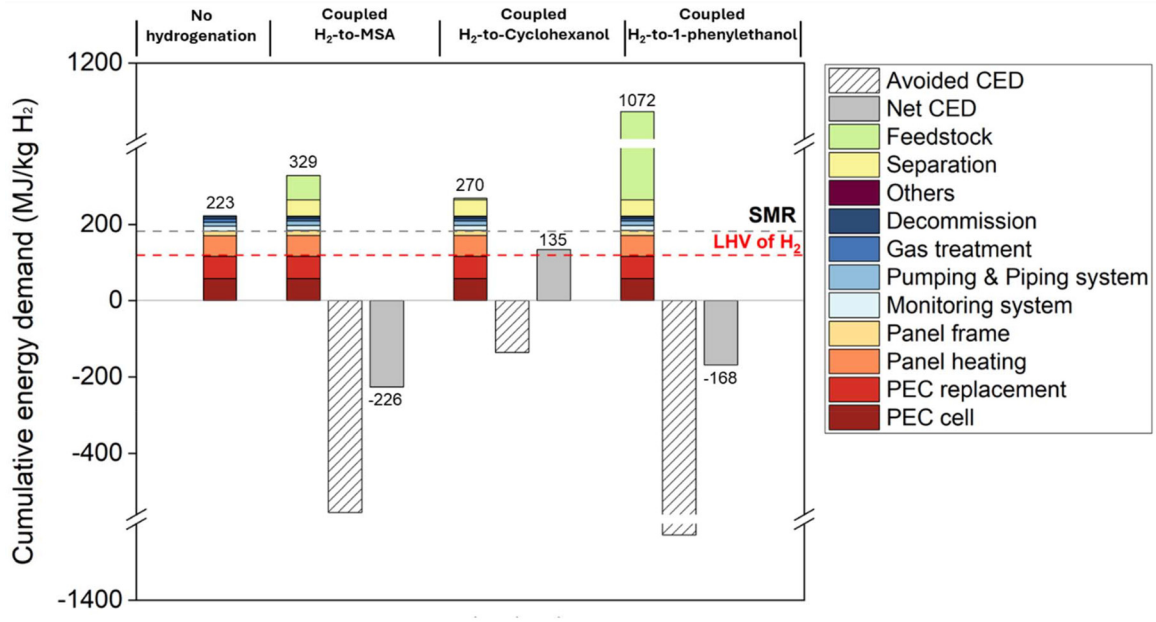

Fig. 4 The cumulative energy demand (CED) of producing H_2 from the coupled PEC hydrogenation system under the base case scenarios for three hydrogenation reactions and when no hydrogenation reaction is coupled. The avoided burdens are shown in shadowed bars, and the grey bars with the labelled values indicate the net CED after the substitution allocation method is applied. The grey dashed line indicates the CED of H_2 from the steam methane reforming method, and the red dashed line indicates the lower heating value of H_2. "Others" includes transportation of PEC devices, operation vehicles, H_2 storage, and water supply.

higher CED because the energy required to hydrogenate acetophenone (806.7 MJ kg^{-1} H_2) is higher than that for the hydrogenation of IA (63.5 MJ kg^{-1} H_2) or phenol (4.7 MJ kg^{-1} H_2). Despite the higher CED, the generation of these chemicals (*i.e.*, MSA, cyclohexanol, and 1-phenylethanol) in a coupled PEC hydrogenation system avoids the energy consumption by the respective conventional production methods. Therefore, the "avoided CED" for each system was determined by developing new processes based on reports of the conventional production of MSA, cyclohexanol, and 1-phenylethanol in SimaPro,[40,80] and the resulting "net CED" could be calculated using eqn (1). The resulting net CED values are −226.1 MJ kg^{-1} H_2, 134.6 MJ kg^{-1} H_2 and −168.0 MJ kg^{-1} H_2 for coupled PEC hydrogenation systems that generate MSA, cyclohexanol and 1-phenylethanol, respectively. In the case of MSA and 1-phenylethanol, the net CED values are negative, indicating that the coupled PEC hydrogenation approach is less energy-intensive than the conventional method. All coupled reactions considered here can produce H_2 at a CED competitive with SMR, although phenol-to-cyclohexanol hydrogenation remains unfavourable when considering the LHV of H_2.

A similar analysis can be extended to determine the GWP of the systems. Fig. 5 shows that the GWP of hydrogen produced in a PEC system without coupled hydrogenation is 12.5 kg CO_2-eq per kg H_2. The value is comparable to or higher than other hydrogen production methods (see Table S1). For example, the GWP of SMR-produced H_2 is 8.5–16.6 kg CO_2-eq per kg H_2;[2,78,81–83] the lower limit is depicted as a grey horizontal dashed line in Fig. 5. Hydrogen production *via* surface/underground coal gasification (SGC/UGC) has a high GWP of 11.3–18 kg CO_2-eq per kg H_2.[84–86] When electrolysis is powered by electricity from the grid, especially if the grid relies heavily on fossil fuels such as coal or natural gas for electricity generation,[87,88] the emissions can be significant at around 31–34 kg CO_2-eq per kg H_2. In contrast, renewable hydrogen has a much lower GWP. For example, biomass-based electrolysis, which utilizes biomass as a feedstock, has a GWP of 3–3.2 kg CO_2-eq per kg H_2.[83,89] The GWP for electrolysis using low-carbon nuclear electricity is around the same range between 1.7 and 4.3 kg CO_2-eq per kg H_2.[83,88,89] Electrolysis using renewable energy such as wind, solar, or hydroelectric power emits around 0.97–9 kg CO_2-eq per kg H_2.[79,83,88,90] When powered by wind energy, electrolysis can be nearly carbon neutral. However, emissions can vary within the given range based on factors such as a high material input at the manufacturing stage of renewable energy devices. Solar photovoltaic-driven electrolysis (PV–EC) produces relatively low levels of GHG emissions, around 4 kg CO_2-eq per kg H_2,[88] as shown as a red horizontal line in Fig. 5. The attributions of the emissions from the PEC and PV–EC can be traced back to the manufacturing process of the PV cells, while SMR emits most of its GHG during plant operation, natural gas production, and distribution. In general, there is only a subtle difference between the distribution of CED and GWP of PEC-produced hydrogen. This suggests that in single-issue LCA, these two parameters are closely related.

At this point we acknowledge that the calculated GWP of our PEC system (12.5 kg CO_2-eq per kg H_2) is 25 times higher com-

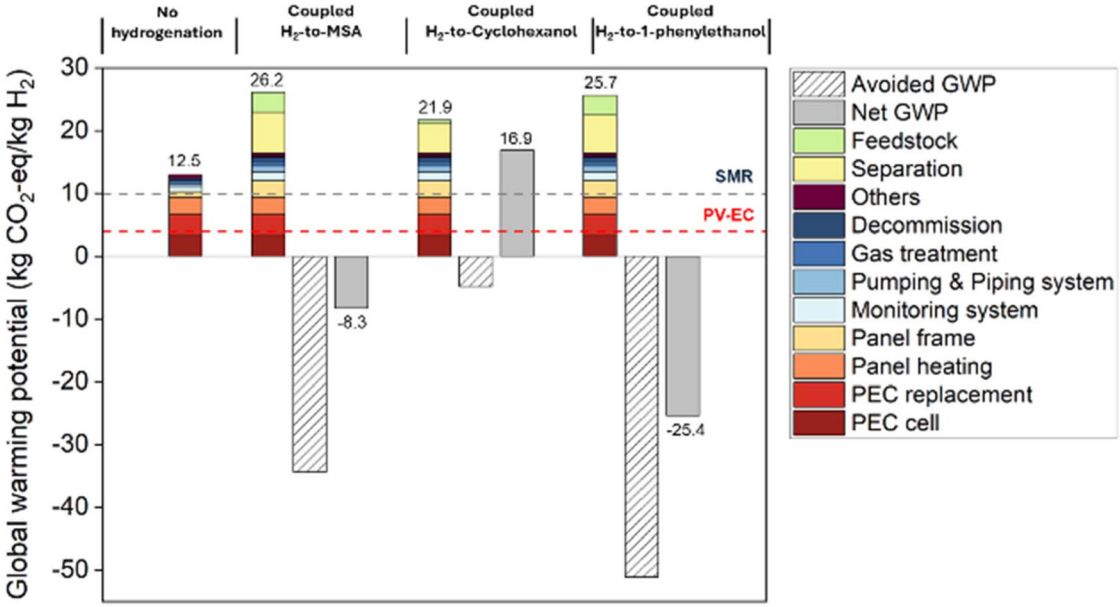

Fig. 5 The global warming potential (GWP) when producing H_2 from the coupled PEC hydrogenation system under the base case scenarios for three hydrogenation reactions and in the absence of coupling to a hydrogenation reaction. The avoided burdens are shown in shadowed bars, and the grey bars with labelled values indicate the net GWP after the substitution allocation method is applied. The grey dashed line indicates the GWP of H_2 from the steam methane reforming method and the red dashed line indicates the GWP of H_2 produced from PV–EC systems. "Others" include transportation of the PEC devices, operation and operational vehicles, H_2 storage, and water supply.

pared to the lowest value reported in other studies for PEC water-splitting devices. For instance, Acar *et al.* reported a GWP value of 0.5 kg CO_2-eq per kg H_2 for PEC water splitting,[91] the lowest and most optimistic among all H_2 production approaches,[92] while another study presented a slightly higher value at 1.16 kg CO_2-eq per kg H_2.[42] These studies unfortunately do not include detailed LCI data for their assumed photoactive materials and/or membranes, but we suspect the discrepancies between these values are related to the different system scale considered. Unlike our analysis, both studies assumed laboratory-scale systems, and the balance of system components required for a larger-scale system are not included.

A similar concept of "avoided GWP" was applied to calculate the "net GWP" of the coupled PEC hydrogenation systems (see eqn (2)). Adding coupled hydrogenation of IA to MSA increases the initial GWP to 26.2 kg CO_2-eq per kg H_2, mainly due to feedstock and separation, but the avoided GWP is much higher. As a result, the net GWP drops to a negative value of −8.3 kg CO_2-eq per kg H_2. This is also the case for the coupled PEC hydrogenation system that generates 1-phenylethanol. Although the initial GWP increases to 25.7 kg CO_2-eq per kg H_2, the avoided GWP is higher, and the net GWP becomes −25.4 kg CO_2-eq per kg H_2. However, the avoided GWP from coupling hydrogenation of phenol to cyclohexanol is less than the extra emissions caused by the feedstock and separation process, which leads to a net GWP of 16.9 CO_2-eq per kg H_2. As a result, this is the only process which was unable to produce H_2 at a competitive GWP with PV–EC or SMR process under the base case scenario.

The comparison between the selected three coupled hydrogenation systems is shown in Table S6. Introducing the coupled hydrogenation reactions in a PEC system to co-generate MSA and 1-phenylethanol can reduce the CED and GWP of H_2 from the system to negative values because the avoided amount of energy and GHG emission is more than the additional inputs from the coupling process, *i.e.*, feedstocks, and separation. Although the coupled hydrogenation of phenol to cyclohexanol requires less CED compared to generation of H_2 only, the reduction is still not enough to make the whole process competitive with SMR. The main reason for this is that the stochiometric coefficient of cyclohexanol to H_2 is 1 : 3, while the stoichiometric coefficient of the other two reactions to H_2 is 1 : 1. Therefore, the required amount of H_2 to produce 1 mole of cyclohexanol is three times higher than that for production of MSA or 1-phenylethanol. Although our previous study revealed the economic benefit of introducing coupled hydrogenation of phenol to cyclohexanol,[17] the higher environmental impact revealed here poses a concern for its implementation. The impact of the economies of scale was further evaluated by comparing the GWP between PEC systems with 1 metric tonne per day (MTD) and 50 MTD hydrogen production capacity (see Note S2). The analysis reveals that scaling effects result in a substantial 68% decrease in GWP emissions per kg hydrogen produced for the 50 MTD PEC system coupled with hydrogenation reactions.

As an additional comparison, we also applied ISO 14404 Step 3 (see Method – LCIA section), which uses economic allocation based on the relative market value of each product. This approach distributes environmental impacts proportionally

according to product prices rather than avoided burdens (see Fig. S1b and Table S7). Under this method, all hydrogenation pathways still show reductions in CED and GWP per kg of H_2 for the coupled system relative to standalone hydrogen production, indicating environmental benefits from integration. However, the environmental performance per kg of chemicals is not necessarily improved. In particular, for the hydrogenation of phenol to cyclohexanol, the allocated CED and GWP rise substantially—to 394.9 MJ kg^{-1} and 17.9 kg CO_2-eq per kg of cyclohexanol, respectively—exceeding the conventional benchmark values (81 MJ kg^{-1} and 2.87 kg CO_2-eq per kg of cyclohexanol). This outcome illustrates that while economic allocation can serve as a useful reference, it may yield skewed results for certain products and should not be the sole basis for evaluating environmental performance.

We briefly note that while SMR and PV–EC outperform PEC in terms of both CED and GWP when only H_2 production is considered, the primary advantage of PEC systems lies in their direct use of solar energy and potential for simplified integration with the coupled hydrogenation reaction. In PEC configurations, hydrogen production and hydrogenation can be spatially and temporally co-located in a single unit, reducing the need for gas purification, compression, and separate reactor infrastructure. It also allows the catalytic hydrogenation to directly benefit from the thermal component of the incident solar energy, something that is not easily possible in PV–EC systems. It was also shown that the H_2-to-MSA conversion in a PV–EC system achieved only 11%, significantly lower than the ~60% conversion observed in PEC system.[18] This performance gap is largely due to mismatched kinetics between hydrogen evolution and homogeneous hydrogenation, as well as the interference of gas bubbles at high current densities in PV–EC systems. Moreover, integrating hydrogenation with SMR or PV–EC requires more complex infrastructure, including a conventional hydrogenation reactor such as a Continuous Stirred Tank Reactor (CSTR). We have performed a preliminary technoeconomic analysis and found that the 10-year operation of a coupled SMR hydrogenation system would result in a levelized cost of MSA (LCOMSA) of $3.00 per kg, while the coupled PEC hydrogenation system could achieve a lower LCOMSA of $2.47 per kg.[17] Finally, we note that the CED and GWP for PEC systems that produce only H_2 are currently limited by the existing manufacturing processes for PEC systems are both energy- and material-intensive. Further optimization of manufacturing techniques and alternative materials is likely to reduce the associated emissions and enhance the overall environmental performance of PEC systems.

Midpoint and endpoint results

We also obtained the LCA results at the midpoint and endpoint levels based on the ReCiPe 2016 method. LCA characterization factors at the midpoint level are located at the point after which the environmental mechanism becomes uniform for all environmental flows under that impact category.[93] Characterization factors at the endpoint level correspond to three areas of protection, *i.e.*, human health, ecosystem quality, and resource scarcity. The midpoint characterization is more closely related to environmental flows. It has relatively low uncertainty, whereas the endpoint characterization provides a better picture of environmental flows to the environment but with more significant uncertainty. The units for all indicators are listed in Table S8.

A total of 16 environmental impact indicators were obtained using the ReCiPe 2016 midpoint approach in SimaPro. Fig. 6 illustrates the contributions of different system components across the impact categories. Notably, in the case of "Global Warming Potential" (GWP), PEC reactors and panel heating exhibit the highest contributions. This breakdown provides actionable insights for targeted system improvements. For instance, reduced GWP can be achieved by replacing the currently considered silicon heterojunction (SHJ) photo absorber with a perovskite-perovskite tandem absorber. This substitution has been reported to significantly reduce greenhouse gas emissions during the fabrication of PEC reactors.[20] In addition, the impact from panel heating—currently powered by mixed-grid electricity—can be mitigated by deploying the system in milder climates where winter temperatures remain above the electrolyte's freezing point, thus eliminating the need for auxiliary heating.

Conversely, the "terrestrial ecotoxicity" impact category reveals a different contribution pattern. Passive components, such as panel frame and monitoring system, instead dominate. This is because these components require substantial amounts of metals (steels, electronic materials), which lead to elevated ecotoxicity. To mitigate this impact, the panel frame design should focus on minimizing steel usage or substituting it with lower-impact alternatives, such as advanced polymers. Moreover, smart control strategies could streamline the monitoring infrastructure, decreasing the number of monitors and sensors required within the system.

To ensure compatibility with conventional and emerging hydrogen production technologies, we conducted a comparative midpoint analysis between our PEC system, the conventional SMR method as the benchmark, and a PV–EC system as the primary competitor for the production of green hydrogen. Although various midpoint indicators are reported in the broader literature, differences in impact categories and units often hinder direct comparison. For instance, Ravilla *et al.* conducted an LCA study on PEC technology, indicating that Ecotoxicity, Human Toxicity, and Ozone Depletion are three metrics where PEC systems exhibit higher impacts compared to PV–EC and SMR.[42] However, the unit conventions used differ from ours and others in the field, making direct cross-study comparison challenging. To maintain consistency and relevance, we focused our comparative analysis on four widely used and consistently reported indicators: global warming potential (kg CO_2-eq per kg H_2), particulates (*i.e.* fine particulate matter with a diameter of 2.5 μm or smaller, in units of kg PM2.5eq per kg H_2), acidification (kg SO_2-eq per kg H_2), and ecotoxicity (kg NO_x-eq per kg H_2).[42,88,94] The results of this comparative assessment are presented in Fig. 7, offering a clear benchmarking of the environmental performance of our

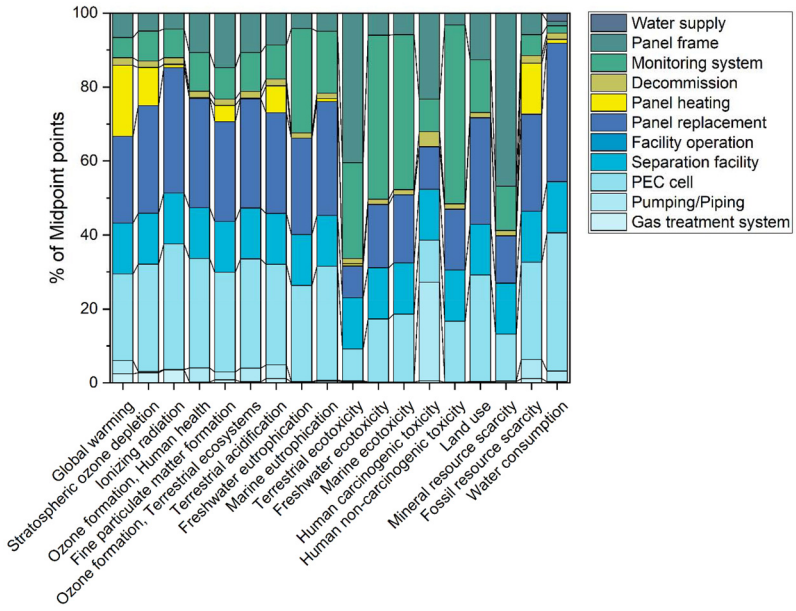

Fig. 6 Midpoint analysis results of the proposed coupled hydrogenation PEC system with the Recipe 2016 method in SimaPro. The percentage distribution of system components is shown for 16 midpoint impact indicators.

PEC system relative to existing technologies. Values for competing H_2 production methods, *i.e.*, SMR and PV–EC, as well as those from another report on a PEC water splitting system are also provided for comparison.[42,88,94] As shown in Fig. 7a, the highest GWP comes from the PEC system coupled with cyclohexanol production (36.4 kg CO_2-eq per kg H_2). This is mainly due to the additional impacts from the hydrogenation process while the avoided impact from the product it produces (cyclohexanol) is insufficient. Coupling the PEC system with H_2-to-MSA shows a significant reduction in GWP; the system has a negative impact (−8.3 kg CO_2-eq per kg H_2) due to the high avoided impact from the current MSA production method, implying a beneficial environmental effect. Fig. 7b shows the particulate matter (PM2.5) emissions. The highest impacts are associated with PV–EC (5.0 kg PM2.5-eq per kg H_2) and SMR (3.0 kg PM2.5-eq per kg H_2). All PEC configurations show zero or slightly negative impacts, indicating potentially beneficial effects on particulate emissions and air pollution. Fig. 7c shows that SMR and PV–EC exhibit high acidification potential (19.0 and 22.0 kg SO_2-eq per kg H_2, respectively). All PEC configurations in this study, especially those coupled with chemical hydrogenation, show zero or even negative impacts. Finally, in terms of ecotoxicity (Fig. 7d), the PEC system reported in the reference study has a significant impact of 48.5 kg NO_x-eq per kg H_2,[42] which may be attributed to the specific electrodes used in that system. SMR and PV–EC each have moderate ecotoxicity impacts (9.0 kg NO_x-eq per kg H_2). The PEC configurations in this study show minimal ecotoxicity impact. In summary, the impacts from the PEC system variants in this study, especially when coupled with MSA, cyclohexanol, or 1-phenylethanol, generally show lower or even negative impacts across multiple categories. This indicates potential environmental benefits compared to the benchmark SMR method, and even PV–EC and PEC systems reported elsewhere.

Next, following the ReCiPe 2016 Endpoint method, the complex midpoint impacts are converted into endpoint indicators representing environmental damage in three broad categories: (i) disability-adjusted life years (DALY) unit for human health, representing the years that are lost or that a person is disabled due to a disease or accident; (ii) species per year (species per year) unit for ecosystem quality, representing the local species loss integrated over time; and (iii) dollar unit (USD 2013) for resources scarcity, representing the extra costs involved for future mineral and fossil resource extraction. Endpoint characterization factors (CF_e) are directly derived from the CF_m (midpoint characterization factors), with a constant midpoint to endpoint factor ($F_{m\to e}$) per impact category using eqn (9).

$$CF_e = CF_m \times F_{m\to e} \quad (9)$$

The endpoint results are shown in Table 1, and all hydrogenation reactions enable the reduction of negative impacts on human health, ecosystems species and resources, while only the H_2-to-cyclohexanol reaction is associated with greater adverse impacts on ecosystem species, whereas the other two reactions mitigate these negative effects.

Sensitivity analysis

The many parameters involved in this LCA introduce uncertainties to the fixed and O&M components of the coupled PEC hydrogenation system. Therefore, sensitivity analysis of these input parameters is necessary. To this end, only few studies have been conducted with large-scale PEC devices, which makes the parameters chosen to be inherently more uncertain.

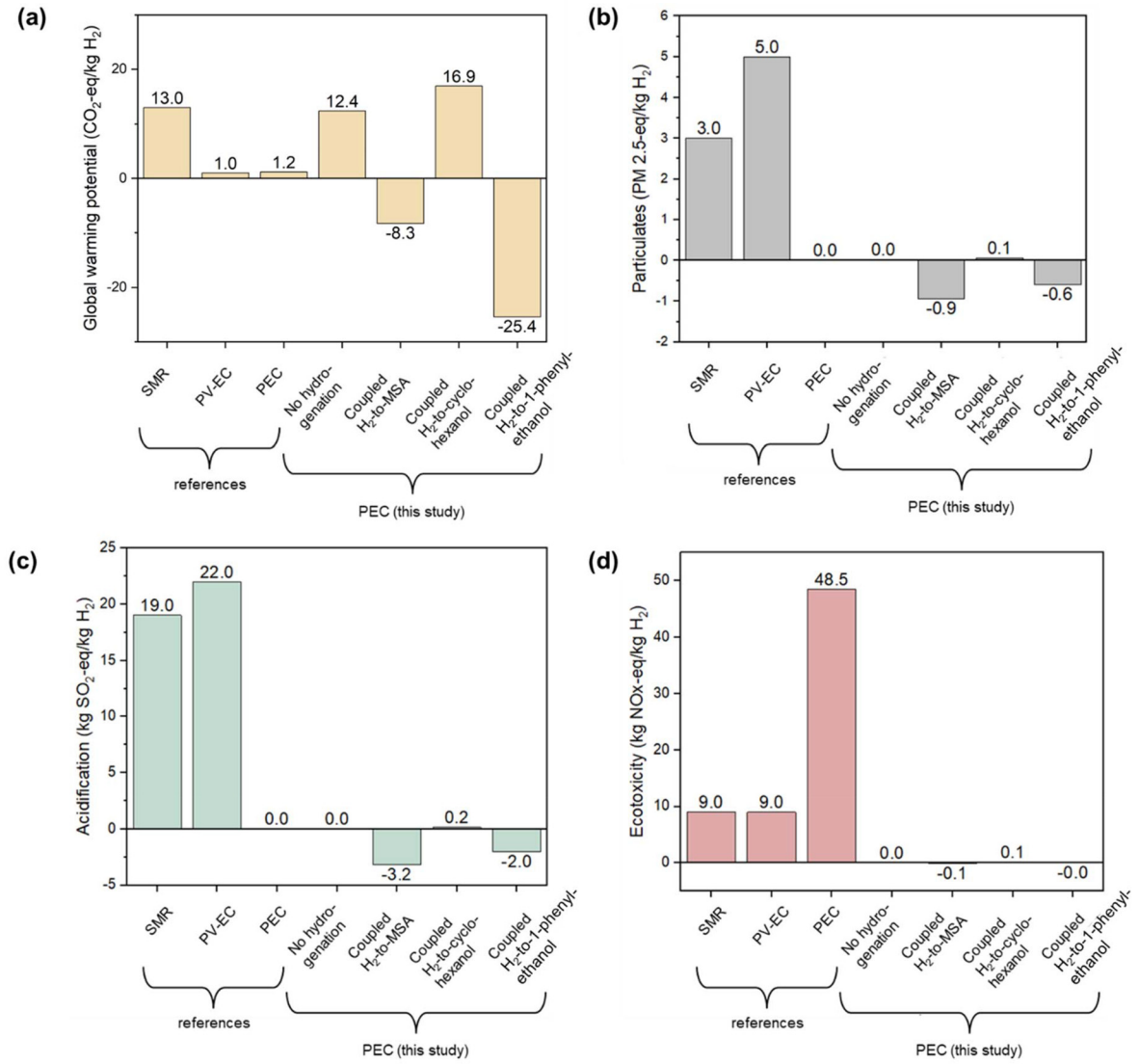

Fig. 7 A comparison of the midpoint impact between LCA results of SMR, PV/EC, PEC from other studies and the LCA results in this study. Our study uses the ReCiPe 2016 impact assessment of 1 kg hydrogen produced within PEC systems when there is no hydrogenation process or coupled with IA to MSA, phenol to cyclohexanol, or acetophenone to 1-phenylethanol. Four common impacts that have been assessed in the literature are included: (a) global warming potential (kg CO_2-eq per kg H_2); (b) particulates (kg PM2.5eq per kg H_2); (c) acidification (kg SO_2-eq per kg H_2); (d) ecotoxicity (kg NO_x-eq per kg H_2).

Table 1 The Recipe 2016 endpoint results of the coupled PEC hydrogenation system

Impact category	Unit	H_2 only	H_2-to-MSA	H_2-to-cyclohexanol	H_2-to-1-phenylethanol
Human health	DaLY	1.5×10^{-3}	-2.7×10^{-2}	0.0	-2.1×10^{-2}
Ecosystems species	species per year	7.9×10^{-5}	-1.1×10^{-3}	4.0×10^{-3}	-8.8×10^{-4}
Resources	USD 2013	3.0×10^{-5}	-1.7×10^{-5}	2.4×10^{-4}	-3.2×10^{-4}

The sensitivity analysis performed here focuses on coupled systems that generate MSA and 1-phenylethanol, since they are economically competitive and environmentally favourable. Three conditions are assumed (*i.e.*, lower, base, and higher cases, see Table S9), and the variation in CED and GWP is calculated accordingly.

The result of the sensitivity analysis for the PEC system coupled with 10% H_2-to-MSA hydrogenation is shown as a tornado plot in Fig. 8. The center point of Fig. 8a represents the CED of H_2 at -226.1 MJ kg^{-1} based on the base case assumptions. Higher values of PEC conversion efficiency (%), H_2-to-MSA conversion (%), system lifetime (years), and the

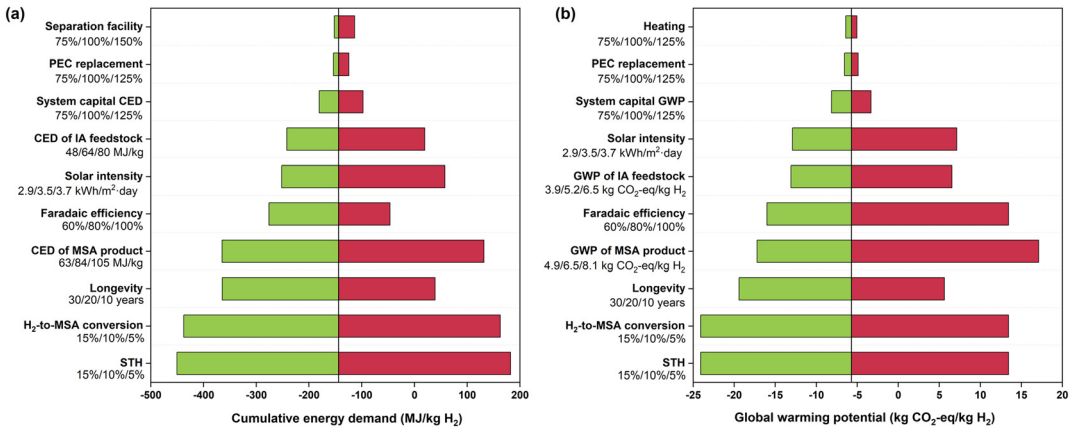

Fig. 8 Perturbative sensitivity analysis of the (a) CED and (b) GWP for the PEC system coupled with IA-to-MSA hydrogenation, for the low, base, and high cases. The center point of the plot (a) and (b) refer to the base case CED of −139.0 MJ kg^{-1} H_2 and the base case GWP of −5.7 kg CO_2-eq per kg H_2.

CED of the MSA product (MJ kg^{-1}) can result in a much better performance. These parameters should be prioritized in the future development of PEC systems to enhance energy efficiency and environmental performance. Moreover, the results highlight a valuable insight: when achieving high STH efficiency and long-term system longevity remains technologically challenging, improving the H_2-to-chemical conversion efficiency can be a more practical and effective approach for optimizing the system than improving the STH efficiency or the system lifetime. The lifetime and the energy content of MSA produced with conventional methods also impose significant impacts on the CED and GWP of H_2. Other parameters (*i.e.*, solar intensity, CED of feedstock, PEC replacement and separation facility) are not able to significantly improve the CED performance of H_2 from the coupled H_2-to-MSA hydrogenation. A range of FE values (60%, 80%, and 100%) is considered for low to high scenarios, which consequently results in a reduced amount of avoided CED. As shown in Fig. 8b, the base case GWP of H_2 is −8.3 kg CO_2-eq per kg. The parameters that impose significant improvement to the GWP reduction are similar to the ones in CED, but the avoided GWP burden by replacing MSA produced from conventional method also plays an important role. The results for other parameters are listed in Table S10. The results for sensitivity analysis for PEC system coupled with H_2-to-1-phenylethanol hydrogenation are similar, as shown in Fig. S6 and Table S11.

Conclusions

In this study, a cradle-to-gate prospective lifecycle analysis (LCA) of a large-scale coupled PEC hydrogenation facility was conducted based on our recently demonstrated laboratory-scale device. Three coupled hydrogenation reactions were selected from our previous technoeconomic analysis study, as they present a positive impact on increasing the economic competitiveness of a PEC system: IA to MSA, phenol to cyclohexanol, and ACP to 1-phenylethanol. This LCA study reveals that the PEC device and utility electricity are the most energy-intensive components of the system. Within the PEC device, the SHJ absorber consumes over 80% of the energy during device manufacturing, which also leads to significant impact on the environment. Regional conditions (Germany in our case) also play a crucial role since a considerable amount of energy is consumed for panel heating when the temperature drops below freezing. The use of electrolytes with lower freezing temperatures may further reduce the CED and GWP since they likely require less heating energy. Most importantly, our LCA study shows that under the base case scenario of 10% STH efficiency and 20 years of longevity, our large-scale PEC system that only generates hydrogen gas is not yet favourable, in terms of its energy balance or environmental impacts, compared with the steam methane reforming (SMR) benchmark. Only when this PEC system is coupled with H_2-to-MSA and H_2-to-1-phenylethanol conversion can it become more favourable; the avoided energy demand and environmental burdens from the hydrogenated products can compensate for the entire life cycle impacts of the system. When only 10% of H_2 is converted to MSA or 1-phenylethanol, negative values of CED and GWP can already be achieved, and even more favourable values can be obtained at higher H_2-to-chemicals conversion. This is not the case when the PEC system is coupled with H_2-to-cyclohexanol. Although coupled PEC hydrogenation of phenol to cyclohexanol has been shown to make the levelized cost of hydrogen (LCOH) competitive in the market,[17] the environmental impacts (GWP) of H_2 generated with this system is almost doubled with the addition of the coupled hydrogenation reaction. Finally, sensitivity analysis shows that the STH efficiency, H_2-to-chemicals conversion, and system longevity are the most influential parameters affecting the energy consumption and GWP emissions over the entire life cycle of the system. The findings offer valuable insights into the future industrial deployment of such systems by identifying the most environmentally favorable chemical reactions. It is important to note,

however, that the selection of chemical production pathways within the system is also influenced by factors such as market demand and evolving green policies, both of which may vary over time. Overall, our study provides a comprehensive evaluation of optimal coupled hydrogenation reactions within a PEC H_2 generation system, demonstrating their potential to significantly enhance system sustainability. By unveiling the environmental advantages of integrating hydrogenation reactions with PEC systems, this work lays a critical foundation for advancing green hydrogen production technologies and fostering innovative pathways toward a more sustainable chemical industry.

Author contributions

Conceptualization, X. Z. and F. F. A.; methodology, X. Z. and F. F. A.; investigation, X. Z.; visualization, X. Z. and F. F. A.; writing—original draft, X. Z.; writing—review & editing, M. S., F. A. A. N., M. R. B, C. S. K. L., R. S., R. v. d. K. and F. F. A.; supervision, R. v. d. K. and F. F. A.; funding acquisition, R. S., R. v. d. K., and F. F. A.

Conflicts of interest

There are no conflicts of interest to declare.

Data availability

The data supporting this study have been included within the article and/or SI. The data supporting this article have been included within the article and as part of the Supplementary Information. See DOI: **https://doi.org/10.1039/d5gc02117k**.

Acknowledgements

This work is supported by the Deutsche Forschungsgemeinschaft (DFG, German Research Foundation) under Germany's Excellence Strategy—EXC 2008/1 (UniSysCat)—390540038 and by the German Helmholtz Association—Excellence Network—ExNet-0024-Phase2-3. X. Z. and F. F. A. acknowledge the Start-up Grant for New Faculty from City University of Hong Kong (Project No. 9610621) and the support from the Research Grants Council (RGC) of Hong Kong through the ANR/RGC Joint Research Scheme (Project A-CityU102/24). This work is also partially funded by the Strategic Seed Fund of City University of Hong Kong (Project No. 7020113). F. A. A. N. acknowledges financial support from Universitas Indonesia through Program Duta Kolaborasi Riset Tahun Anggaran 2024 No. NKB-749/UN2.RST/HKP.05.00/2024.

References

1 M. Rosental, T. Fröhlich and A. Liebich, *Front. Clim.*, 2020, **2**, 586199.
2 IEA, *The Future of Hydrogen: Seizing today's opportunities*, 2019.
3 G. H. Patel, J. Havukainen, M. Horttanainen, R. Soukka and M. Tuomaala, *Green Chem.*, 2024, **26**, 992–1006.
4 J. Jia, L. C. Seitz, J. D. Benck, Y. Huo, Y. Chen, J. W. D. Ng, T. Bilir, J. S. Harris and T. F. Jaramillo, *Nat. Commun.*, 2016, **7**, 1–6.
5 M. E. Ivanova, R. Peters, M. Müller, S. Haas, M. F. Seidler, G. Mutschke, K. Eckert, P. Röse, S. Calnan and R. Bagacki, *Angew. Chem., Int. Ed.*, 2023, **62**, e202218850.
6 W.-H. Cheng, M. H. Richter, M. M. May, J. Ohlmann, D. Lackner, F. Dimroth, T. Hannappel, H. A. Atwater and H.-J. Lewerenz, *ACS Energy Lett.*, 2018, **3**, 1795–1800.
7 A. M. Fehr, A. Agrawal, F. Mandani, C. L. Conrad, Q. Jiang, S. Y. Park, O. Alley, B. Li, S. Sidhik and I. Metcalf, *Nat. Commun.*, 2023, **14**, 3797.
8 M. R. Shaner, H. A. Atwater, N. S. Lewis and E. W. McFarland, *Energy Environ. Sci.*, 2016, **9**, 2354–2371.
9 A. Sharma, T. Longden, K. Catchpole and F. J. Beck, *Energy Environ. Sci.*, 2023, **16**, 4486–4501.
10 B. A. Pinaud, J. D. Benck, L. C. Seitz, A. J. Forman, Z. Chen, T. G. Deutsch, B. D. James, K. N. Baum, G. N. Baum and S. Ardo, *Energy Environ. Sci.*, 2013, **6**, 1983–2002.
11 T. Grube, J. Reul, M. Reuß, S. Calnan, N. Monnerie, R. Schlatmann, C. Sattler, M. Robinius and D. Stolten, *Sustainable Energy Fuels*, 2020, **4**, 5818–5834.
12 S. K. Ngoh and D. Njomo, *Renewable Sustainable Energy Rev.*, 2012, **16**, 6782–6792.
13 C. Acar and I. Dincer, *Int. J. Hydrogen Energy*, 2014, **39**, 1–12.
14 B. Mei, G. Mul and B. Seger, *Adv. Sustainable Syst.*, 2017, **1**, 1600035.
15 H. Luo, J. Barrio, N. Sunny, A. Li, L. Steier, N. Shah, I. E. Stephens and M. M. Titirici, *Adv. Energy Mater.*, 2021, **11**, 2101180.
16 D. F. S. Morais, L. M. G. Sena, J. M. Ribeiro, T. da S. Lopes, P. Dias, A. Mendes, C. A. E. Costa, A. E. Rodrigues, S. R. S. Pereira, P. C. Pinto, R. A. R. Boaventura, C. J. Tavares, V. J. P. Vilar and F. C. Moreira, *Green Chem.*, 2025, **27**, 6537–6555.
17 X. Zhang, Z. Li, L. R. Sinaga, M. Schwarze, R. Schomäcker, R. van de Krol and F. F. Abdi, *ACS Sustainable Chem. Eng.*, 2024, **12**, 13783–13797.
18 K. Obata, M. Schwarze, T. A. Thiel, X. Zhang, B. Radhakrishnan, I. Y. Ahmet, R. van de Krol, R. Schomäcker and F. F. Abdi, *Nat. Commun.*, 2023, **14**, 6017.
19 B. D. James, G. N. Baum, J. Perez and K. N. Baum, *DOE report*, 2009.
20 X. Zhang, M. Schwarze, R. Schomäcker, R. van de Krol and F. F. Abdi, *Nat. Commun.*, 2023, **14**, 991.
21 S. Collins, Y. Acevedo, D. V. Esposito, R. B. Chandran, S. Ardo, B. D. James and H. Breunig, *Energy Environ. Sci.*, 2025, **18**, 6690–6700.

22 M. Finkbeiner, A. Inaba, R. Tan, K. Christiansen and H.-J. Klüppel, *Int. J. Life Cycle Assess.*, 2006, **11**, 80–85.
23 A. Zimmermann, L. Müller, Y. Wang, T. Langhorst, J. Wunderlich, A. Marxen, K. Armstrong, G. Buchner, A. Kätelhön and M. Bachmann, *Techno-Economic Assessment & Life Cycle Assessment Guidelines for CO2 Utilization (Version 1.1)*, 2020.
24 J. Verduyckt and D. E. De Vos, *Chem. Sci.*, 2017, **8**, 2616–2620.
25 Y. Wu, C. Gao, Y. Ren, C. Wang and J. Xu, *China Pat.*, CN102617326, 2012.
26 H. Shi, W. Shen and H. Xu, *China Pat.*, CN1609089A, 2004.
27 K. Sasaki, A. Kunai, J. Harada and S. Nakabori, *Electrochim. Acta*, 1983, **28**, 671–674.
28 U. Sanyal, J. Lopez-Ruiz, A. B. Padmaperuma, J. Holladay and O. Y. Gutiérrez, *Org. Process Res. Dev.*, 2018, **22**, 1590–1598.
29 G. Wernet, C. Bauer, B. Steubing, J. Reinhard, E. Moreno-Ruiz and B. Weidema, *Int. J. Life Cycle Assess.*, 2016, **21**, 1218–1230.
30 Pré Consultants, *SimaPro Database Manual: Methods Library*, 2020.
31 T. Stocker, *Climate change 2013: the physical science basis: Working Group I contribution to the Fifth assessment report of the Intergovernmental Panel on Climate Change*, Cambridge University press, 2014.
32 M. A. Huijbregts, Z. J. Steinmann, P. M. Elshout, G. Stam, F. Verones, M. D. Vieira, A. Hollander, M. Zijp and R. van Zelm, *ReCiPe 2016: a harmonized life cycle impact assessment method at midpoint and endpoint level report I: characterization*, 2016.
33 Deutscher Wetterdienst, Global, diffuse and direct radiation (monthly and annual totals and deviations), **https://www.dwd.de/EN/ourservices/solarenergy/maps_globalradiation_sum_new.html**, (accessed 12/2024).
34 T. Huld, R. Müller and A. Gambardella, *Sol. Energy*, 2012, **86**, 1803–1815.
35 Germany - Producer prices in industry: Water collection, treatment and supply, **https://tradingeconomics.com/germany/producer-prices-in-industry-water-collection-treatment-supply-eurostat-data.html**, (accessed 12/2024).
36 Germany Electricity Price, **https://tradingeconomics.com/germany/electricity-price**, (accessed 12/2024).
37 KITCO, Platinum spot price, **https://www.kitco.com/charts/interactive-charts/?Symbol=PLATINUM&Currency=USD&multiCurrency=true&langId=EN&period=2329200000&utm_source=kitco&utm_medium=banner&utm_content=20110407_iCharts_182day_platinum_link&utm_campaign=iCharts**, (accessed 12/2024).
38 Public Net Electricity Generation 2023 in Germany: Renewables Cover the Majority of the Electricity Consumption for the First Time, **https://www.ise.fraunhofer.de/en/press-media/press-releases/2024/public-electricity-generation-2023-renewable-energies-cover-the-majority-of-german-electricity-consumption-for-the-first-time.html#:~:text=In%202023%2C%20renewables%20accounted%20for,the%20socket)%20was%2057.1%20percent**, (accessed 12/2024).
39 K. Obata, M. Schwarze, T. A. Thiel, X. Zhang, B. Radhakrishnan, I. Y. Ahmet, R. van de Krol, R. Schomäcker and F. F. Abdi, *Nat. Commun.*, 2023, **14**, 6017.
40 M. Villalba, M. del Pozo and E. J. Calvo, *Electrochim. Acta*, 2015, **164**, 125–131.
41 Y. Song, S. H. Chia, U. Sanyal, O. Y. Gutiérrez and J. A. Lercher, *J. Catal.*, 2016, **344**, 263–272.
42 A. Ravilla, Z. Song, Y. Yan, I. Celik, *IEEE 52nd Photovoltaic Specialist Conference (PVSC)*, Seattle, 2024, pp. 377–380.
43 I. Y. Ahmet, Y. Ma, J.-W. Jang, T. Henschel, B. Stannowski, T. Lopes, A. Vilanova, A. Mendes, F. F. Abdi and R. van de Krol, *Sustainable Energy Fuels*, 2019, **3**, 2366–2379.
44 R. Sathre, C. D. Scown, W. R. Morrow, J. C. Stevens, I. D. Sharp, J. W. Ager, K. Walczak, F. A. Houle and J. B. Greenblatt, *Energy Environ. Sci.*, 2014, **7**, 3264–3278.
45 A. Diehl, Determining Module Inter-Row Spacing, **https://www.greentechrenewables.com/article/determining-module-inter-row-spacing**, (accessed 12/2023).
46 Z. Liu, M. Peters, V. Shanmugam, Y. S. Khoo, S. Guo, R. Stangl, A. G. Aberle and J. Wong, *Sol. Energy Mater. Sol. Cells*, 2016, **144**, 523–531.
47 A. Louwen, W. Van Sark, R. Schropp, W. Turkenburg and A. Faaij, *Prog. Photovolt.: Res. Appl.*, 2015, **23**, 1406–1428.
48 F. F. Abdi and R. van de Krol, *J. Phys. Chem. C*, 2012, **116**, 9398–9404.
49 E. Sánchez-Cruces, E. Barrera-Calva, K. Lavanderos and F. González, *Energy Procedia*, 2014, **57**, 2812–2818.
50 P. Zhai, S. Haussener, J. Ager, R. Sathre, K. Walczak, J. Greenblatt and T. McKone, *Energy Environ. Sci.*, 2013, **6**, 2380–2389.
51 L. Duclos, M. Lupsea, G. Mandil, L. Svecova, P.-X. Thivel and V. Laforest, *J. Cleaner Prod.*, 2017, **142**, 2618–2628.
52 D. Jones, *Polymer electrolyte membrane and direct methanol fuel cell technology*, 2012, pp. 27–56.
53 P. Zhai and E. D. Williams, *Environ. Sci. Technol.*, 2010, **44**, 7950–7955.
54 H. Kim and V. Fthenakis, *Prog. Photovolt.: Res. Appl.*, 2011, **19**, 228–239.
55 E. Alsema, *Energy requirements of thin-film solar cell modules—a review*, Report 1364-0321, 1998.
56 P. Treenate, N. Limphitakphong and O. Chavalparit, *IOP Conf. Ser.: Mater. Sci. Eng.*, 2017, **222**, 012010.
57 S. Haussener, C. Xiang, J. M. Spurgeon, S. Ardo, N. S. Lewis and A. Z. Weber, *Energy Environ. Sci.*, 2012, **5**, 9922–9935.
58 S. Hayter, S. Tanner, E. Urbatsch and J. Zuboy, *US Department of Energy, National Renewable Energy Laboratory (NREL)*, Federal Energy Managment Program (FEMP), 2004.
59 Wasserhaus, Platinumwasser NEO-7 Reverse Osmosis System, **https://www.wasserhaus.de/epages/62372559.sf/en_GB/?ViewObjectPath=%2FShops%2F62372559%2FProducts%2F13244**, (accessed 12/2024).
60 S. Shanmuganathan, M. Johir, A. Listowski, S. Vigneswaran and J. Kandasamy, *Proc. Environ. Sci.*, 2016, **35**, 930–937.
61 J. Macknick, R. Newmark, G. Heath and K. C. Hallett, *Environ. Res. Lett.*, 2012, **7**, 045802.

62 AxFlow, Kreiselpumpe mit Peripherallaufrad, Pedrollo PQ-PRO, **https://www.axflow24.de/home/Kreiselpumpe-mit-Peripherallaufrad-Pedrollo-PQ-PRO-230V-p224372875**, (accessed 12/2024).
63 A. Plappally, *Renewable Sustainable Energy Rev.*, 2012, **16**, 4818–4848.
64 J. E. Pope, *Rules of thumb for mechanical engineers*, Elsevier, 1996.
65 J. Koornneef, T. van Keulen, A. Faaij and W. Turkenburg, *Int. J. Greenhouse Gas Control*, 2008, **2**, 448–467.
66 C. Yang and J. Ogden, *Int. J. Hydrogen Energy*, 2007, **32**, 268–286.
67 M. S. Peters and K. D. Timmerhaus, *Plant design and economics for chemical engineers*, McGraw-Hill International, 2018.
68 E. Weiszflog and M. Abbas, *Life Cycle Assessment of Hydrogen Storage Systems for Trucks An assessment of environmental impacts and recycling flows of carbon fiber*, 2022.
69 M. A. Weiss, J. B. Heywood, E. M. Drake, A. Schafer and F. F. AuYeung, *On the Road in 2020: A life-cycle analysis of new automobile technologies*, 2000.
70 D. Wetterdienst, Climatological maps of Germany, **https://www.dwd.de/EN/ourservices/klimakartendeutschland/klimakartendeutschland.html**, (accessed 12/2023).
71 J. Greenblatt, *Photo-electrochemical Hydrogen Plants at Scale: A Life-cycle Net Energy Assessment*, The Royal Society of Chemistry, 2019.
72 Mettler Toledo, Continuous Stirred Tank Reactors (CSTRs), **https://www.mt.com/de/en/home/products/L1_AutochemProducts/Chemical-Synthesis-and-Process-Development-Lab-Reactors/continuous-stirred-tank-reactors-cstr.html?cmp=sea_01010123&SE=GOOGLE&Campaign=MT_AC_EN_ROW&Adgroup=CSTR&bookedkeyword=continuous%20stirred%20tank%20reactors&matchtype=p&adtext=560327130691&placement=&network=g&kclid=_k_Cj0KCQjw852XBhC6ARIsAJsFPN0eiN9M4L4vN2KXbD1J6-7uLu1qbCGU00Ky7YbQ2k7OMHWRwfT9NqwaAnTzEALw_wcB_k_&cq_src=google_ads&cq_cmp=243074089&cq_con=120737852063&cq_term=continuous%20stirred%20tank%20reactors&cq_med=&cq_plac=&cq_net=g&cq_pos=&cq_plt=gp&gclid=Cj0KCQjw852XBhC6ARIsAJsFPN0eiN9M4L4vN2KXbD1J6-7uLu1qbCGU00Ky7YbQ2k7OMHWRwfT9NqwaAnTzEALw_wcB**, (accessed 12/2024).
73 Continuous stirred tank reactors (cstrs) **https://amarequip.com/flow-reactor-services-products/continuous-stirred-tank-reactor**, (accessed 11/2024).
74 M. Schwarze, *Chem. Ing. Tech.*, 2021, **93**, 31–41.
75 M. Schmidt, S. Schreiber, L. Franz, H. Langhoff, A. Farhang, M. Horstmann, H.-J. Drexler, D. Heller and M. Schwarze, *Ind. Eng. Chem. Res.*, 2018, **58**, 2445–2453.
76 A. Bavley and C. J. Knuth, *USA Pat.*, US-2773897-A, 1956.
77 Ç. Efe, L. A. van der Wielen and A. J. Straathof, *Biomass Bioenergy*, 2013, **56**, 479–492.
78 P. L. Spath and M. K. Mann, *Life cycle assessment of hydrogen production via natural gas steam reforming*, National Renewable Energy Lab. (NREL), Golden, CO (United States), 2000.
79 M. Mann and P. Spath, *Life cycle assessment of renewable hydrogen production via wind/electrolysis: Milestone completion report*, National Renewable Energy Lab., Golden, CO. (US), 2004.
80 S. A. Akhade, N. Singh, O. Y. Gutiérrez, J. Lopez-Ruiz, H. Wang, J. D. Holladay, Y. Liu, A. Karkamkar, R. S. Weber and A. B. Padmaperuma, *Chem. Rev.*, 2020, **120**, 11370–11419.
81 I. Dincer, *Int. J. Energy Res.*, 2007, **31**, 29–55.
82 C. Antonini, K. Treyer, A. Streb, M. van der Spek, C. Bauer and M. Mazzotti, *Sustainable Energy Fuels*, 2020, **4**, 2967–2986.
83 A. Ozbilen, I. Dincer and M. A. Rosen, *Int. J. Hydrogen Energy*, 2011, **36**, 11321–11327.
84 A. Verma and A. Kumar, *Appl. Energy*, 2015, **147**, 556–568.
85 E. Cetinkaya, I. Dincer and G. F. Naterer, *Int. J. Hydrogen Energy*, 2012, **37**, 2071–2080.
86 A. Midilli, H. Kucuk, M. E. Topal, U. Akbulut and I. Dincer, *Int. J. Hydrogen Energy*, 2021, **46**, 25385–25412.
87 C. Wulf and M. Kaltschmitt, *Int. J. Hydrogen Energy*, 2012, **37**, 16711–16721.
88 A. Simons and C. Bauer, in *Transition to Hydrogen: Pathways toward Clean Transportation*, ed. Wokaun and A., Wilhelm, E., 2011, 13–57.
89 V. Utgikar and T. Thiesen, *Int. J. Hydrogen Energy*, 2006, **31**, 939–944.
90 C. Koroneos, A. Dompros, G. Roumbas and N. Moussiopoulos, *Int. J. Hydrogen Energy*, 2004, **29**, 1443–1450.
91 C. Acar and I. Dincer, *Int. J. Hydrogen Energy*, 2022, **47**, 40118–40137.
92 A. Vilanova, P. Dias, T. Lopes and A. Mendes, *Chem. Soc. Rev.*, 2024, **53**, 2388–2434.
93 M. Goedkoop, R. Heijungs, M. Huijbregts, A. De Schryver, J. Struijs and R. Van Zelm, *A life cycle impact assessment method which comprises harmonised category indicators at the midpoint and the endpoint level*, 2009, vol. 1, pp. 1–126.
94 S. Sadeghi and S. Ghandehariun, *Int. J. Hydrogen Energy*, 2023, **48**, 19326–19339.

